GeroScience
https://doi.org/10.1007/s11357-026-02325-5

ORIGINAL ARTICLE

Abnormal periodic and aperiodic resting-state electroencephalographic markers in Lewy body and Alzheimer's diseases with cognitive decline

Matteo Carpi · Antonio Pio Afragola · Mina De Bartolo · Susanna Lopez · Burcu Bölükbaş · Claudio Del Percio · Veronica Henao Isaza · Roberta Lizio · Giuseppe Noce · Lorenc Barjami · Filippo Carducci · Andrea Soricelli · Marco Salvatore · Franco Giubilei · Bahar Güntekin · Görsev Yener · Federico Massa · Dario Arnaldi · Francesco Famà · Matteo Pardini · Raffaele Ferri · Bartolo Lanuzza · Fabrizio Stocchi · Laura Vacca · Chiara Coletti · Moira Marizzoni · John Paul Taylor · Lutfu Hanoğlu · Harun Yırıkoğulları · Giovanni B. Frisoni · Sofia Cuoco · Paolo Barone · Marianna Amboni · Arianna Cappiello · Laura Bonanni · Anita D'Anselmo · Roberta Biundo · Simone Cauzzo · Eleonora Fiorenzato · Angelo Antonini · Fabrizia D'Antonio · Giuseppe Bruno · Francesco Infarinato · Paola Romano · Simone Marziali · Maria Francesca De Pandis · Claudio Babiloni

Received: 18 December 2025 / Accepted: 13 May 2026
© The Author(s) 2026

Abstract Lewy body disease (LBD) and Alzheimer's disease (AD) are the most common causes of cognitive decline and dementia and are associated with characteristic alterations in resting-state electroencephalographic (rsEEG) activity. This multicenter exploratory study investigated periodic and aperiodic rsEEG features in patients with cognitive decline due to Lewy body disease (LBCD) and Alzheimer's disease (ADCD), compared with cognitively unimpaired older adults (Nold), and examined the clinical relevance of these markers in LBCD. A

Supplementary information The online version contains supplementary material available at https://doi.org/10.1007/s11357-026-02325-5.

M. Carpi · A. P. Afragola · M. De Bartolo · S. Lopez · B. Bölükbaş · C. Del Percio · V. Henao Isaza · R. Lizio · L. Barjami · F. Carducci · C. Babiloni (✉)
Department of Physiology and Pharmacology, Vittorio Erspamer", Sapienza University of Rome, P. Le A. Moro 5, Rome 00185, Italy
e-mail: claudio.babiloni@uniroma1.it

R. Lizio · F. Carducci
Oasi Research Institute - IRCCS, Troina, Italy

G. Noce · A. Soricelli · M. Salvatore · R. Ferri · B. Lanuzza · P. Barone
IRCCS Synlab SDN, Naples, Italy

A. Soricelli
Department of Medical, Movement and Well-Being Sciences, University of Naples Parthenope, Naples, Italy

F. Giubilei
Department of Neuroscience, Mental Health, and Sensory Organs, Sapienza University of Rome, Rome, Italy

B. Güntekin
Department of Biophysics, School of Medicine, Istanbul Medipol University, Istanbul, Turkey

B. Güntekin · L. Hanoğlu · H. Yırıkoğulları
Research Institute for Health Sciences and Technologies (SABITA), Neuroscience Research Center, Istanbul Medipol University, Istanbul, Turkey

G. Yener
Department of Neurology, Faculty of Medicine, Dokuz Eylül University, Izmir, Turkey

G. Yener
IBG: International Biomedicine and Genome Center, Izmir, Turkey

F. Massa · D. Arnaldi · F. Famà · M. Pardini
Dipartimento Di Neuroscienze, Oftalmologia, Genetica, Riabilitazione e Scienze Materno-Infantili (DiNOGMI), Università Di Genova, Genoa, Italy

Published online: 22 May 2026

total of 140 LBCD, 135 ADCD, and 118 Nold datasets from the PDWAVES archive underwent spectral parameterization to decompose rsEEG power spectra (1–30 Hz) into periodic peaks and aperiodic background activity. Both clinical groups showed a significant slowing of the individual alpha frequency (IAF), more pronounced in LBCD, along with reduced periodic alpha and beta power reflected in a lower vigilance index. The aperiodic exponent was elevated in both groups, and the aperiodic offset was also higher in LBCD, suggesting steeper spectral profiles consistent with increased inhibitory cortical tone. Within the LBCD group, poorer cognition was associated with higher low-frequency alpha power, whereas better cognition was predicted by higher high-frequency alpha power. A reduced vigilance index was associated with the presence of visual hallucinations, while no associations emerged for other symptoms. These findings suggest that combined periodic and aperiodic rsEEG features may provide relevant markers of altered vigilance regulation in LBCD. Future studies should evaluate whether these EEG markers can inform targeted interventions, such as neuromodulatory or audiovisual stimulation, to stabilize quiet-vigilance states and improve clinical outcomes.

Graphical abstract Panel A shows the spectral parameterization of rsEEG activity into periodic and aperiodic components. Panel B summarizes the main group differences in key rsEEG markers across LBCD, ADCD, and Nold participants. Panel C shows the topographical associations between the vigilance index and cognition and visual hallucinations in LBCD; colors reflect the direction and strength of the associations. For the visual hallucinations map, negative log-odds indicate lower odds of hallucinations for higher vigilance index values, whereas positive log-odds indicate higher odds; values around ± 1.5 correspond approximately to odds ratios of 0.22 and 4.5, respectively. Abbreviations: rsEEG, resting-state electroencephalography; LBCD, cognitive decline due to Lewy body disease; ADCD, cognitive decline due to Alzheimer's disease; Nold, cognitively unimpaired older adults; IAF, individual alpha frequency; MMSE, Mini-Mental State Examination; *p*,

F. Massa · D. Arnaldi · F. Famà · M. Pardini
IRCCS Ospedale Policlinico San Martino, Genoa, Italy

F. Stocchi · L. Vacca · C. Coletti · F. Infarinato · P. Romano · S. Marziali
IRCCS San Raffaele Roma, Rome, Italy

F. Stocchi · M. F. De Pandis
San Raffaele Open University, Rome, Italy

M. Marizzoni
Biological Psychiatry Unit, IRCCS Istituto Centro San Giovanni Di Dio Fatebenefratelli, Brescia, Italy

J. P. Taylor
Translational and Clinical Research Institute, Faculty of Medical Sciences, Newcastle University, Newcastle Upon Tyne, UK

L. Hanoğlu · H. Yırıkoğulları
Department of Neurology, School of Medicine, Istanbul Medipol University, Istanbul, Turkey

G. B. Frisoni
Memory Center, Department of Rehabilitation and Geriatrics, University Hospitals and University of Geneva, Geneva, Switzerland

G. B. Frisoni
Laboratory of Neuroimaging of Aging (LANVIE), University of Geneva, Geneva, Switzerland

S. Cuoco · P. Barone · M. Amboni · A. Cappiello
Department of Medicine, Surgery and Dentistry "Scuola Medica Salernitana", Neuroscience Section, University of Salerno, Baronissi, Italy

L. Bonanni · A. D'Anselmo
Department of Aging Medicine and Sciences, University "G. d'Annunzio" of Chieti-Pescara, Chieti, Italy

R. Biundo
Department of General Psychology, University of Padua, Padua, Italy

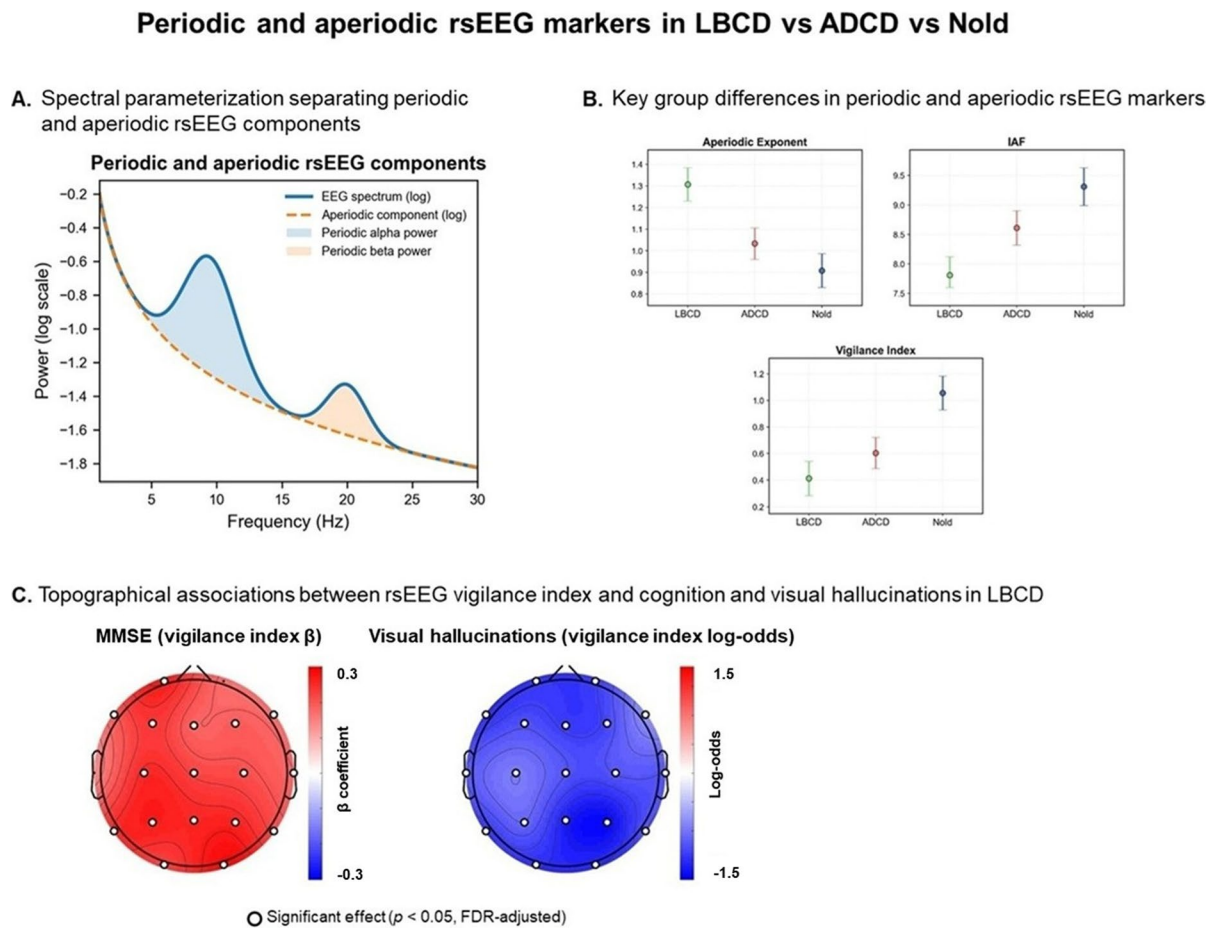
R. Biundo · A. Antonini
IRCCS, San Camillo Hospital, Venice, Italy

R. Biundo · S. Cauzzo · E. Fiorenzato · A. Antonini
Parkinson and Movement Disorders Unit, Study Center for Neurodegeneration (CESNE), Department of Neuroscience, Padua Neuroscience Center (PNC), University of Padua, Padua, Italy

F. D'Antonio · G. Bruno
Department of Human Neurosciences, Sapienza University of Rome, Rome, Italy

S. Marziali · M. F. De Pandis · C. Babiloni
Hospital San Raffaele Cassino, Cassino, FR, Italy

standardized regression coefficient; log-odds, logistic regression coefficient.



Keywords Lewy body disease (LBD) · Alzheimer's disease (AD) · Cognitive decline · Resting-state EEG · Periodic and aperiodic components · Vigilance regulation

Introduction

Lewy body disease (LBD) and Alzheimer's disease (AD) are the most common age-related neurodegenerative conditions leading to progressive cognitive decline and dementia [1, 2]. Although clinical guidelines prioritize neuropsychological evaluations and standardized rating scales for assessing cognitive impairment, the identification of reliable biomarkers remains essential for prevention, early diagnosis, and optimization of disease-modifying interventions.

In Alzheimer's disease with cognitive decline (ADCD), etiological diagnosis is based on cerebrospinal fluid (CSF) markers and positron emission tomography (PET) evidence of amyloid-β and tau pathology, while structural magnetic resonance imaging (MRI) contributes critically to monitoring neurodegeneration [3, 4]. In contrast, a definitive neurobiological diagnosis of LBD with cognitive decline (LBCD) remains challenging because in vivo detection of Lewy bodies, which are primarily composed of aggregated α-synuclein and ubiquitin, is currently unfeasible [5, 6]. Diagnosis, therefore, relies on clinical core features, specifically recurrent

visual hallucinations, persistent cognitive fluctuations in attention and alertness, and rapid eye movement (REM) sleep behavior disorder (RBD). This clinical assessment can be complemented by indicative biomarkers such as dopamine transporter (DAT) imaging via single-photon emission computed tomography (SPECT) or positron emission tomography (PET), iodine-123 MIBG myocardial scintigraphy, and polysomnographic confirmation of RBD [5, 6]. Supportive diagnostic elements include occipital or cingulate hypometabolism or hypoperfusion on SPECT/PET, relatively preserved medial temporal lobe volume on MRI, and increased delta (<4 Hz) and theta/pre-alpha (4–7 Hz) resting-state electroencephalographic (rsEEG) power [5].

Notably, rsEEG abnormalities are a commonly observed yet often underrecognized feature of both LBCD and ADCD, possibly reflecting impaired regulation of quiet vigilance states that characterize both the prodromal stage of mild cognitive impairment (MCI) and dementia [7, 8]. In fact, across several studies, patients with ADCD and LBCD have been repeatedly characterized by increased slow-frequency power and a shift of the dominant alpha peak toward lower frequencies (≤8 Hz), coupled with markedly reduced posterior alpha power [9–11].

More recently, research on AD and LBD has begun to examine the contribution of the aperiodic component of rsEEG power spectra, conceptualized as non-oscillatory background neural activity with a characteristic 1/*f*-like decay. Periodic rsEEG peaks (such as those in the alpha or beta ranges) are superimposed on this broadband background, which decreases gradually with increasing frequency [12, 13]. By applying spectral decomposition methods such as the *specparam* algorithm (formerly known as FOOOF, i.e., fitting oscillations and one over f), periodic and aperiodic spectral features can be dissociated and quantified independently [12].

From a neurophysiological perspective, the periodic and aperiodic components of rsEEG power spectra convey distinct but complementary information that may be relevant for neurodegenerative diseases. Periodic oscillatory peaks reflect the synchronous activity of thalamocortical and cortical circuits that regulate quiet vigilance and sensorimotor gating in idling mode [7, 14–16]. Conversely, the aperiodic exponent (i.e., spectral slope) is generally believed to reflect large-scale excitation-inhibition (E/I) balance, with steeper slopes suggesting increased inhibitory tone and/or reduced excitatory activity [17–19]. In turn, the aperiodic offset (i.e., the intercept of the broadband component) has been associated with neuronal firing rates and synaptic input and shows meaningful correlations with resting-state blood oxygen level-dependent (BOLD) functional MRI [20, 21]. Together, these parameters provide a neurophysiological proxy for cortical metabolic activity and arousal levels.

In a growing number of studies, the *specparam* algorithm and alternative spectral parameterization method (e.g., irregular resampling auto-spectral analysis; [22]) have been successfully applied to characterize age-related rsEEG aperiodic changes in cognitively unimpaired older adults as well as in patients with ADCD, LBCD, and related disorders [23–30]. Furthermore, results obtained using this approach have demonstrated good test–retest reliability [31, 32] and robustness to mathematical harmonization accounting for the confounding effects of different equipment and procedures in multicenter studies [25].

Across this literature, separating periodic and aperiodic rsEEG components has helped clarify age-related and disease-related alterations beyond what can be inferred from raw power spectra. For instance, after correcting for aperiodic activity, the periodic alpha peak tends to appear slower in older adults relative to younger participants. At the same time, its absolute amplitude often remains comparable across age groups [28]. Other studies applying spectral decomposition methods have also identified alterations in periodic alpha power and in composite oscillatory indices (e.g., beta-to-theta ratios) in ADCD [23, 25, 26], as well as disease-specific changes in aperiodic spectral features in LBCD, ADCD, and Parkinson's disease with cognitive deficits (PDCD) [24, 25, 27, 29, 30]. Specifically, LBCD patients showed a markedly steeper aperiodic component relative to cognitively unimpaired individuals, MCI patients, ADCD patients, PDCD patients, and individuals with frontotemporal dementia [25, 29]. Furthermore, similar increases in aperiodic exponent and offset have been observed in PDCD compared to controls, regardless of dopaminergic therapy [27], and both the exponent and offset have been found to be elevated in ADCD relative to frontotemporal dementia, with widespread scalp topographies [25, 30].

Taken together, these findings suggest that ADCD and LBCD present distinct rsEEG spectral alterations. ADCD is characterized by reduced periodic alpha power (~8–10 Hz), particularly over posterior cortical areas. In contrast, LBCD is marked by relatively widespread elevations in slow oscillatory frequencies (theta/pre-alpha range, ~4–6 Hz) and significant increases in aperiodic spectral parameters (exponent and offset). However, despite this evidence, the spatial distribution of periodic and aperiodic features across these conditions and their clinical significance remain poorly understood.

To address these gaps, the present exploratory study examined periodic-aperiodic spectral differences between LBCD, ADCD, and cognitively unimpaired elderly (Nold) participants in a large, well-characterized multicenter cohort. The primary objective was to clarify the neurophysiological mechanisms underlying rsEEG slowing in LBCD and ADCD by decomposing EEG spectra into periodic oscillatory peaks and aperiodic background activity. A second objective was to investigate the relationship between these EEG markers, cognitive status, and characteristic clinical symptoms in LBCD, with a particular focus on those reflecting disturbances in the regulation of quiet vigilance.

Based on prior evidence suggesting that aperiodic components, as indices of cortical E/I balance and arousal, may be more altered in LBCD than in ADCD, we expected group differences in the aperiodic exponent and offset, alongside periodic differences consistent with the reviewed literature. By contrast, given the limited neurophysiological characterization of these relationships to date, the associations between rsEEG markers and clinical manifestations in LBCD were examined with a purely exploratory approach.

Materials and methods

Participants and overall study design

Participants for this study were retrospectively included from the PDWAVES Consortium archive (https://www.pdwaves.eu/). Clinical and rsEEG datasets were available for 142 LBCD, 139 ADCD, and 119 Nold participants. Due to suboptimal model fit in the parameterization procedure described below, seven participants were excluded (two LBCD, four ADCD, and one Nold), resulting in a final sample of 140 LBCD, 135 ADCD, and 118 Nold individuals.

Minimum sample size for the main analyses was established through an a priori power analysis conducted using G*Power 3.1 [33]. Assuming an analysis of covariance with fixed effects, main effects, and interactions (three groups and three covariates) as a conservative proxy of our principal inferential procedures based on linear mixed models, we targeted a small-to-medium effect size (partial eta-squared [η_p^2] around 0.03, corresponding to Cohen's $f = 0.17$). This value was deliberately chosen to be smaller than an effect previously estimated ($\eta_p^2 = 0.31$) in a previous study investigating differences in EEG current densities between patients with dementia due to AD or LBD and controls [9]. With this effect size, a significance level of $\alpha = 0.05$, and power = 0.80, the required sample size was $N = 337$, which was exceeded in this study ($N = 393$) to accommodate inherent complexity of the statistical design.

Regarding diagnostic procedures and inclusion criteria, participants in the LBCD group underwent neurological and clinical examination and received a diagnosis of probable LBD based on consensus guidelines (i.e., presence of two core clinical features among recurrent visual hallucinations, cognitive fluctuations with variations in attention and alertness, and RBD, or one core clinical feature corroborated by one validated disease biomarker) [5, 6]. Visual hallucinations were assessed with the second item of the Neuropsychiatric Inventory (NPI) [34]; cognitive fluctuations were evaluated with the standardized Clinician Assessment of Fluctuations (CAF) [35]; and the probable diagnosis of RBD was made according to patient and caregiver reports consistent with the International Classification of Sleep Disorders, Third Edition (ICSD-3) [36]. In the present study, each of these three symptoms was coded as a binary variable (present = 1, absent = 0). Motor symptoms and cardinal features of parkinsonism were assessed using the Movement Disorder Society-updated Unified Parkinson's Disease Rating Scale – part III (UPDRS-III) [37], yielding a total score ranging from 0 to 108. Notably, 37 LBCD participants (26.4%) underwent SPECT/PET imaging showing reduced dopamine transporter (DAT) reuptake, considered an indicative biomarker for LBD [5]. Exclusion criteria for LBCD participants included major systemic diseases;

evidence of vascular dementia; participation in clinical trials using disease-modifying drugs; current or past major psychiatric disorders (e.g., major depressive disorder or substance use disorder according to DSM-5; [38]); neurological illnesses not related to cognitive decline; past or present diagnosis of epilepsy or history of seizures; and current use of antiepileptic medications.

Participants in the ADCD group also underwent medical examination and were diagnosed with Alzheimer's disease based on clinical evidence consistent with both the National Institute of Neurological Disorders and Stroke-Alzheimer Disease and Related Disorders (NINCDS-ADRDA) working group criteria [39] and DSM-5 diagnostic criteria [38]. Exclusion criteria for ADCD participants included major systemic diseases; current or past major psychiatric disorders; neurological illnesses not related to cognitive decline; current participation in clinical trials involving disease-modifying drugs; and chronic use of medications with anticholinergic, sedative, hypnotic, antipsychotic, or centrally acting analgesic properties. Use of antiparkinsonian drugs was not permitted, while acetylcholinesterase inhibitors and memantine were allowed. Past or current diagnosis of epilepsy, previous seizures, and use of antiepileptics were additional exclusion criteria.

In both cognitive decline groups, dementia or MCI was diagnosed according to DSM-5 criteria for major and mild neurocognitive disorders. Dementia required evidence of significant cognitive decline in at least one cognitive domain from neuropsychological assessment accompanied by clinically relevant impairment in instrumental and/or basic activities of daily living. MCI required evidence of cognitive decline in at least one domain in the absence of significant functional impairment. In this study, Mini-Mental State Examination (MMSE) [40] score (0–30 range, with lower score indicating worse cognitive status) is reported as a global summary index of cognitive functioning.

Nold participants underwent clinical and neurological examination as well as cognitive screening to confirm the absence of cognitive decline (MMSE $\geq$ 27). Exclusion criteria were consistent with those applied to the LBCD and ADCD groups and included systemic diseases (e.g., diabetes), past or current psychiatric or neurological disorders, and chronic use of psychoactive medications.

Table 1 reports demographic and clinical characteristics of the final sample. As expected, MMSE scores were significantly lower in both clinical groups compared with Nold. LBCD and ADCD participants were older and had a lower degree of education than Nold; sex distribution also differed across groups, with a higher proportion of males in the LBCD group. Regarding cognitive status, 7.1% of LBCD participants and 22.2% of ADCD participants were diagnosed with MCI, the latter being significantly more frequent. The percentage of participants using LBD- or AD-related medications (i.e., antiparkinsonian agents, cholinergic agonists, and psychotropic drugs) is summarized in Table S1 in the Supplementary Materials.

As described in the following section, all participants underwent rsEEG recordings in a controlled experimental setting. Written informed consent was obtained prior to study inclusion, and procedures

Table 1 Demographic and clinical characteristics of participants with cognitive decline due to Lewy body disease (LBCD), cognitive decline due to Alzheimer's disease (ADCD), and cognitively unimpaired older adults (Nold). Values are presented as mean ± standard deviation unless otherwise specified

Variable	LBCD ($N=140$)	ADCD ($N=135$)	Nold ($N=118$)	Statistical test	Post hoc
Age	75.2 ± 6.9	74.4 ± 7.4	68.9 ± 8.1	ANOVA, $p<0.001$	LBDC > Nold; ADCD > Nold
Sex (F/M)	52/90	73/66	70/49	χ^2, $p<0.001$	–
Education	8.0 ± 4.2	10.1 ± 5.0	12.4 ± 4.7	ANOVA, $p<0.001$	LBCD < Nold; LBDC < ADCD; ADCD < Nold
MMSE	20.4 ± 5.7	21.3 ± 5.4	28.9 ± 1.3	Kruskal–Wallis test, $p<.0001$	LBCD < Nold; ADCD < Nold
MCI *n* (%)	10 (7.1)	30 (22.2)	–	χ^2, $p<0.001$	–

ADCD cognitive decline due to Alzheimer's disease, *LBCD* cognitive decline due to Lewy body disease, *Nold* cognitively unimpaired older adults, *MCI* mild cognitive impairment, *MMSE* Mini-Mental State Examination

were conducted in accordance with the Declaration of Helsinki. The ethical committees of all participating PDWAVES Consortium units approved the study protocol.

rsEEG recording protocol

EEG recordings were conducted at all sites with participants seated in a comfortable reclined chair in a quiet, dimly lit room. To minimize fatigue and homeostatic sleep pressure, sessions were scheduled in the morning. Participants who were regularly taking medication were asked to delay administration until after the EEG session to reduce the acute pharmacological effects on rsEEG activity.

Each session consisted of two consecutive conditions lasting approximately 3 to 5 min each: an eyes-closed resting-state condition and an eyes-open resting-state condition. For the present study, only the eyes-closed condition was analyzed. Before recording, participants received standardized instructions describing the two conditions and were asked to remain relaxed, refrain from speaking or performing large voluntary movements, and allow their mind to wander while avoiding structured mental activity. If experimenters observed behavioral or EEG indicators of drowsiness or sleep onset (e.g., vertex sharp transients, K-complexes, or sleep spindles), they gently encouraged participants to remain awake in order to preserve the intended recording state.

Each recording center used its own EEG system applying acquisition parameters that minimized aliasing artifacts. Analog band-pass filters ranged between 0.01 and 60 Hz or 0.01 and 100 Hz, and sampling rates varied from 128 to 1024 Hz across units (see Table S2 in the Supplementary Materials for unit-specific information regarding included participants and employed EEG sampling rate). These parameters provided an adequate spectral resolution for the frequency ranges of interest—namely, the delta (< 4 Hz), theta (~ 4–7 Hz), alpha (~ 8–12 Hz), and beta (~ 14–30 Hz) bands.

All recordings used a standard monopolar 19-channel montage based on the international 10–20 system (Fp1, Fp2, F7, F3, Fz, F4, F8, T7, C3, Cz, C4, T8, P7, P3, Pz, P4, P8, O1, O2). A frontal electrode served as ground, and cephalic or linked-earlobe references were used according to local protocols. Vertical and horizontal ocular activity (e.g., eye blinks, eye movements) was monitored through two electrooculogram (EOG) channels (0.3–70 Hz band-pass). Impedances for all recording electrodes were kept below 5 kΩ.

Preliminary analysis of rsEEG data

EEG data were centrally analyzed by expert researchers at the Sapienza University of Rome unit of the PDWAVES Consortium. The preprocessing pipeline was designed to optimize signal quality and minimize recording artifacts, following the guidelines of an expert workgroup of the International Federation of Clinical Neurophysiology [41]. The same procedures have been previously adopted and validated in rsEEG studies by our group across different clinical populations [9, 42, 43] and are briefly summarized below.

Raw EEG recordings were imported and processed using the EEGLAB toolbox (v2022.1) [44] within the MATLAB environment (R2022a; MathWorks, Natick, MA, USA). Preprocessing steps aimed to identify and eliminate channels with persistent artifacts (e.g., poor scalp contact), EEG segments with widespread contamination, and independent components associated with non-neural sources.

Two experimenters independently performed a visual inspection of each EEG trace to detect electrodes or segments displaying continuous, irreparable artifacts. In cases of disagreement, a third expert was consulted. No more than three channels (approximately one-sixth of the montage) were removed per participant at this stage and missing channels were reconstructed using EEGLAB's interpolation tool based on neighboring electrodes.

Subsequently, three experts visually reviewed each recording to identify and reject segments affected by muscle activity, ocular artifacts, head movements, or other recognizable non-physiological noise sources.

As a final cleaning step, independent component analysis (ICA) was applied to isolate residual non-neural activity [45, 46]. Components corresponding to blinking, eye movements, muscle activity, or cardiac artifacts were removed based on consensus visual inspection of their characteristic topographies and spectral properties. No more than five components were rejected per participant. After ICA decomposition and component rejection, a final visual quality check of the EEG traces was carried out.

The artifact-free EEG data were segmented into two-second epochs, band-pass filtered between 1 and 40 Hz, downsampled to 128 Hz when the original sampling rate was higher, and re-referenced to the common average across all electrodes.

Analysis of rsEEG power spectral density and spectral parameterization

Artifact-free rsEEG epochs from the eyes-closed condition were used to compute power spectral density (PSD). The *pop_spectopo* function in EEGLAB was applied using a window length equal to the sampling rate (i.e., 1-s Hanning window, no overlap), yielding a frequency resolution of 1 Hz. For each electrode, absolute rsEEG spectral power values were obtained for each integer frequency bin from 1 to 30 Hz and used as input for the subsequent analysis of periodic (oscillatory peaks) and aperiodic components.

Spectral parameterization was conducted using the *specparam* algorithm (https://specparam-tools.github.io/) [12]. Consistent with previous work and with the expected characteristics of resting-state spectra, the following settings were applied: fixed mode (i.e., no "knee" parameter), PSD peak width limits from 0.5 to 8 Hz, a maximum of 5 peaks, a minimum peak height of 0 (arbitrary units), and a peak "elevation" threshold of 1.5 (arbitrary units). With these parameters, the algorithm decomposed each electrode's rsEEG power spectrum (1–30 Hz) into a broadband aperiodic component and superimposed periodic peaks. Model fit was assessed using the explained variance (R^2) provided by the algorithm. For each participant, the mean R^2 across all electrodes was computed, and values below 0.95 were considered suboptimal; participants not meeting this criterion were excluded from further analyses.

The aperiodic component was modeled as a decreasing $1/f^{\chi}$ function in log–log power × frequency space, where the exponent χ reflects the steepness (negative slope) of the spectrum from 1 to 30 Hz. Aperiodic offset values (log-power intercepts) were also extracted. Concurrently, periodic components were modeled as Gaussian-shaped peaks rising above the aperiodic background [12].

For each electrode, the modeled aperiodic rsEEG power spectrum was then subtracted from the log-transformed raw rsEEG power spectrum to generate aperiodic-corrected rsEEG power values (arbitrary units), reflecting the residual narrowband power relative to the model-fitted aperiodic component.

Because alpha rhythms typically exhibit a posterior scalp distribution [47, 48], power peaks identified by *specparam* at electrodes P3, Pz, P4, O1, and O2 within the 6–14 Hz broad alpha range were used to estimate the individual alpha frequency (IAF), defined as the frequency bin showing the maximum aperiodic-corrected rsEEG power among posterior electrodes [49]. Similarly, the individual beta frequency (IBF) was identified as the frequency with the largest detected power peak within the beta range (14–22 Hz) across all electrodes. Aperiodic-corrected rsEEG power values at IAF and IBF were extracted for each electrode.

Two individualized alpha bands were then defined around the IAF: a low-alpha band (IAF − 2 Hz to IAF) and a high-alpha band (IAF to IAF + 2 Hz). Aperiodic-corrected power in each band was computed as the mean residual power across all frequency bins within the corresponding window. Additionally, aperiodic-corrected delta power was computed as the mean residual power across 1–3 Hz. Since aperiodic-corrected subtraction may yield negative values in this range (reflecting dominance of the aperiodic background), delta power was interpreted as a delta residual after removal of the aperiodic component.

Finally, a synthetic vigilance index was derived at the electrode level as the ratio between aperiodic-corrected power at the alpha and beta peaks (i.e., rsEEG power at IAF and IBF) and aperiodic-corrected power at slow frequencies (positive residuals only), using the following formula:

$$\text{VigilanceIndex} = \log_{10} \frac{IAF_{\text{Power}} + IBF_{\text{Power}}}{\sum_{i=1}^{5} \max\left(rsEEG_{\text{Power}iHz}, 0\right)}$$

This index was designed to summarize the balance between faster periodic rsEEG rhythms typically associated with stable quiet wakefulness (i.e., alpha- and beta-range activity) and slower-frequency activity associated with reduced vigilance and drowsiness, in line with previous EEG-vigilance work and ratio-based spectral indices [50–52], as well as with established models of wakefulness-to-sleep onset transitions, in which posterior alpha dominance characterizes relaxed wakefulness, whereas the emergence of diffuse theta and slower rhythms marks the transition toward lower arousal levels and early light

sleep [53–56]. Hence, higher vigilance index values indicate a relative predominance of faster wake-related rsEEG activity, whereas lower values reflect a shift toward slower-frequency activity and reduced quiet vigilance.

The following rsEEG-derived variables were then retained for subsequent analyses: (1) aperiodic-corrected power at IAF; (2) aperiodic-corrected power at IBF; (3) aperiodic-corrected low-alpha power; (4) aperiodic-corrected high-alpha power; (5) aperiodic-corrected delta residual power; (6) periodic vigilance index; (7) aperiodic exponent; and (8) aperiodic offset. Each variable was retained at the single-electrode level, and also summarized as a global scalp average and as an average over posterior electrodes (P7, P3, Pz, P4, P8, O1, O2).

Statistical analyses

Single-electrode topographic scalp maps and aggregated data were used to analyze periodic and aperiodic rsEEG parameters. Statistical analyses, computational procedures, and plotting were performed using jamovi (v2.5.6, including the GAMLj3 module for linear models) [57, 58], R (v4.5.1) [59], MATLAB (R2022a; MathWorks, Natick, MA, USA), Python (v3.13.1), and GraphPad Prism (v8.0.1, GraphPad Software, Boston, MA, USA).

Descriptive statistics were summarized as counts and percentages for categorical variables and as means and standard deviations (or standard errors of the mean) for continuous variables. Between-group differences in demographic and clinical variables were examined with one-way ANOVA or the Kruskal–Wallis test depending on distributional assumptions, whereas chi-squared (χ^2) tests were used for comparisons of categorical proportions. Bivariate associations between variables were examined using Pearson's correlations, Spearman's rank correlations, or point-biserial correlations based on the measurement level of the variables. Statistical significance was set at $p < 0.05$ for all analyses unless otherwise specified.

Preliminary comparisons of global aperiodic-corrected rsEEG power spectra shapes across the three groups were performed using bin-by-bin permutation-based pairwise testing. For each integer frequency bin between 1 and 30 Hz, Welch's t statistic was computed for each pairwise contrast (LBCD vs. Nold, ADCD vs. Nold, LBCD vs. ADCD). To preserve potential site effects, nonparametric p-values were generated using unit-stratified label permutations, whereby group labels were permuted within each recording unit while bin-wise rsEEG power values remained fixed. For each frequency bin, two-sided permutation p-values were calculated as the proportion of $|t_{perm}| \geq |t_{obs}|$ across 5000 permutations. Benjamini–Hochberg false discovery rate (FDR) correction [60] was applied across the 30 bins within each pairwise comparison, with significance defined as FDR-adjusted $p < 0.05$.

Main statistical analyses included two stages: (1) comparisons between the three diagnostic groups in rsEEG parameters, and (2) follow-up analyses of associations between rsEEG parameters and clinical outcomes within the LBCD group.

To assess group differences in rsEEG variables (i.e., IAF and IBF frequencies, periodic components, and aperiodic parameters), linear mixed models (LMMs) were fitted separately for global averages and posterior regional averages (the latter selected due to the known posterior distribution of rsEEG characteristic rhythms). Eight LMMs were estimated in total. All models included age, sex, and years of education as a priori covariates, given their documented associations with rsEEG spectral measures and cognitive functioning in aging and neurodegenerative populations [13, 61, 62]. Recording unit was entered as a random intercept to account for variability related to equipment and acquisition protocols. Prior to modeling, distributional shapes of all dependent variables were examined, and no major deviations from a Gaussian distribution were observed (skewness and kurtosis values fell within the acceptable ranges of −1 to 1 and −3 to 3, respectively [63, 64]).

For each LMM, partial eta-squared (η_p^2) values were computed to quantify the effect size of group differences. Estimated marginal means with 95% confidence intervals were extracted for visualization and for planned post hoc contrasts. When a significant group effect was detected, pairwise differences were evaluated using FDR-corrected p-values.

As a supplementary sensitivity analysis addressing age differences between groups, and specifically to rule out age-related effects involving the control group that may be relevant in quantitative EEG analyses [13], the primary LMMs were repeated using an age-restricted Nold subsample obtained by progressively excluding

the youngest cognitively unimpaired participants in 1-year steps, while retaining sex and years of education as covariates and recording unit as a random intercept. The final threshold was selected as the smallest age cutoff yielding both a non-significant omnibus age difference across groups in a one-way ANOVA and acceptable pairwise age balance (i.e., standardized mean differences) relative to the two clinical groups.

Clinical follow-up analyses in the LBCD group examined the associations between rsEEG predictors (restricted to those variables showing significant group effects) and clinical outcomes. Linear regression models were used for continuous outcomes, and binomial logistic regression models were used for binary outcomes. All models included age, sex, and education as covariates, and regression assumptions were checked by examining variance inflation factors, visual inspection of residuals Q-Q plots, and Durbin-Watson statistics close to 2, indicating the absence of problematic multicollinearity, deviations from normality, or residual autocorrelation. Predictor significance was evaluated using t statistics for linear regression and Z statistics for logistic regression. For logistic models, odds ratios with 95% confidence intervals were reported, with statistical significance defined as a confidence interval not including 1. Standardized regression coefficients (β) were computed for all linear models.

To complement these large-scale analyses, topographic mapping was used to visualize both group differences and regression results. For between-group comparisons, electrode-wise distributions of EEG periodic and aperiodic components were displayed in scalp maps, and pairwise differences between groups were inspected using electrode-by-electrode t-tests with FDR correction. For single-group regression analyses, scalp maps showed electrode-level regression coefficients (controlling for age, sex, and education), and electrodes surviving FDR correction were highlighted to identify possible spatial clusters associated with clinical outcomes.

Results

rsEEG power spectra across groups

After excluding seven participants whose mean model fit fell below the predefined *specparam* quality threshold of 0.95, overall spectral parameterization performance was excellent across the final sample (mean $R^2 = 0.99$; range 0.96–0.998; mean fit error = 0.05; range 0.02–0.10). Figure 1A shows group-mean raw rsEEG power spectra averaged across all scalp electrodes ("global") and their aperiodic fit curves, whereas Fig. 1B shows group-mean aperiodic-corrected global rsEEG power spectra. As visible in Fig. 1B, compared with the Nold participants, both clinical groups (LBCD and ADCD) exhibited lower aperiodic-corrected global rsEEG power in the alpha and beta bands. Detailed inspection of the global rsEEG alpha peak revealed a marked attenuation of alpha power in ADCD, while LBCD showed only a modest reduction but a clear slowing of the peak's central frequency (i.e., lower IAF). These distinctions were less apparent in the raw (uncorrected) global rsEEG power spectra (Fig. 1A), likely reflecting relevant between-group differences in the broadband rsEEG aperiodic component that masked oscillatory variability.

These descriptive differences were formally tested using permutation-based pairwise comparisons (Fig. 1C–E). Compared to the Nold group, the LBCD group showed significantly reduced corrected rsEEG power in the 1–2 Hz range, increased power in the 4–7 Hz range, and decreased power in both the 9–12 Hz and 16–26 Hz ranges (Fig. 1C). Furthermore, the ADCD group, relative to Nold, displayed significantly increased rsEEG power in the 3–7 Hz range and decreased power in the 9–12 Hz, 15–26 Hz, and 29–30 Hz ranges (Fig. 1D). Finally, in the direct LBCD vs. ADCD comparison, the ADCD group showed significantly lower corrected rsEEG power in the 4–8 Hz range (Fig. 1E). All reported frequency-specific differences survived FDR correction at $p < 0.05$.

Group differences in periodic and aperiodic rsEEG spectral features

LMMs tested group differences for all rsEEG variables of interest, and the estimated marginal means for each parameter across groups are shown in Fig. 2. The *specparam* algorithm did not detect an rsEEG alpha power peak for one participant (ADCD) and an rsEEG beta power peak for 16 participants (11 LBCD; 5 ADCD). Accordingly, analyses involving IAF, IBF, and their derived measures were conducted with this

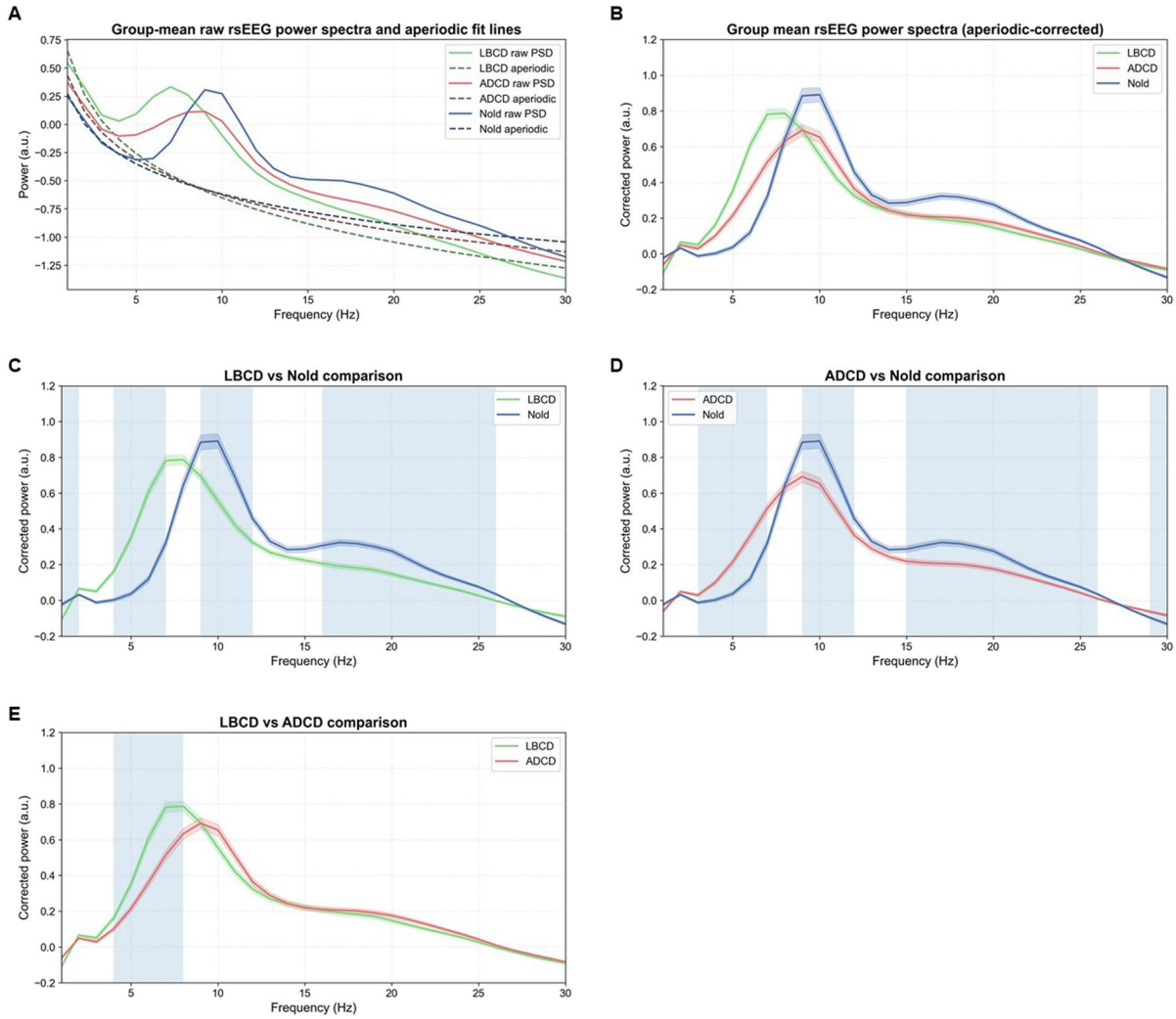
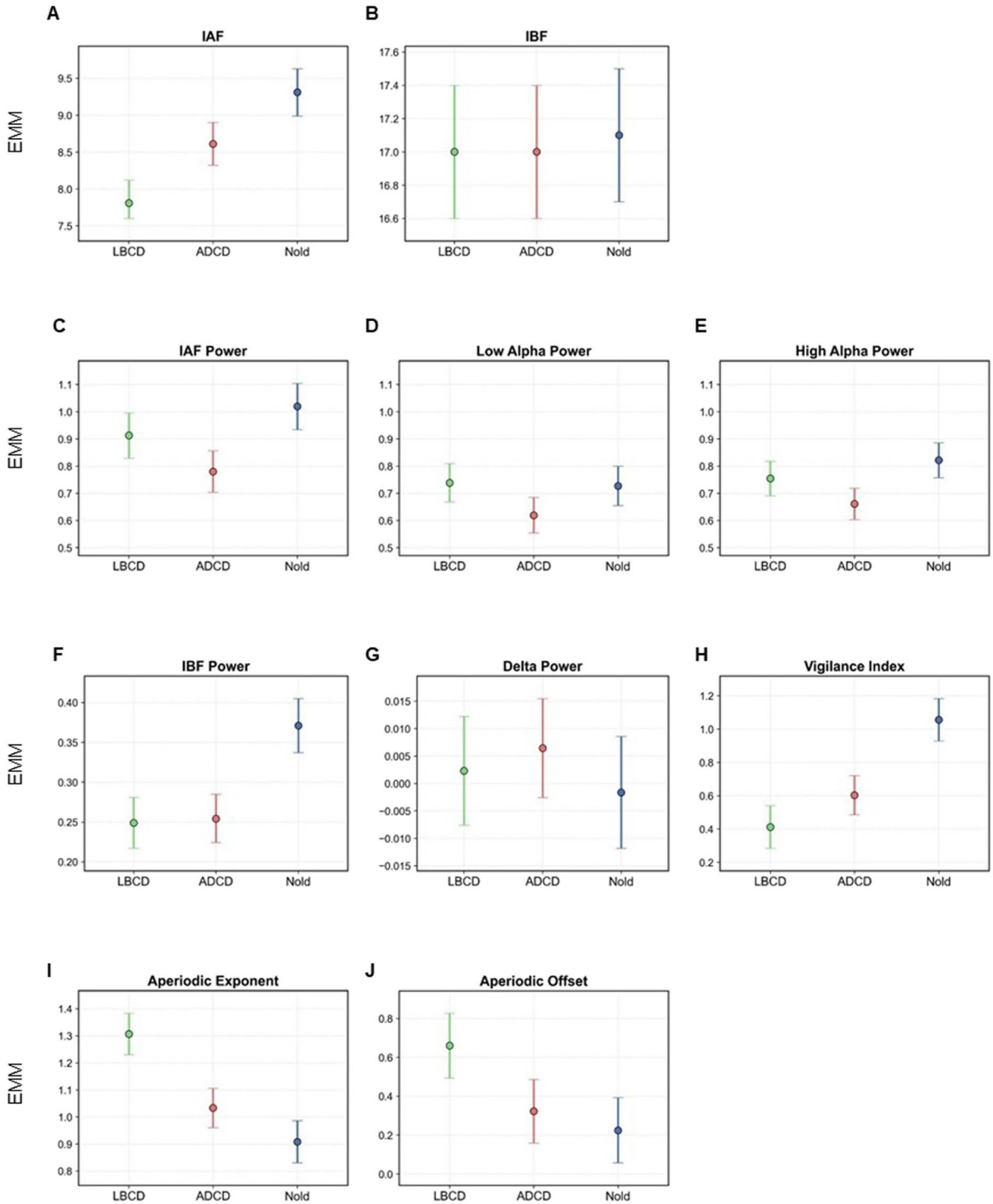


Fig. 1 Grand-mean resting-state EEG (rsEEG) power spectra in participants with cognitive decline due to Lewy body disease (LBCD), cognitive decline due to Alzheimer's disease (ADCD), and cognitively unimpaired older adults (Nold). **A** Raw rsEEG power spectra (solid lines) and corresponding aperiodic fit curves (dashed) across the 1–30 Hz frequency range. **B** Aperiodic-corrected rsEEG power spectra (raw rsEEG power spectra minus the aperiodic fit) for the three groups; shaded areas show the standard error of the mean. **C–E** Pairwise comparisons of aperiodic-corrected rsEEG power spectra for each group contrast. Blue shaded regions indicate frequency bins in which groups significantly differed based on permutation testing ($p < 0.05$, false discovery rate-adjusted). a.u., arbitrary units: rsEEG, resting-state electroencephalography

limited amount of missing data. A significant group effect was found for the IAF ($p < 0.001$, $\eta_p^2 = 0.29$). Specifically, the IAF was lower in the LBCD group compared to both the Nold (mean difference = 1.5, FDR-adjusted $p < 0.001$) and the ADCD group (mean difference = 0.8, FDR-adjusted $p < 0.001$), and lower in ADCD compared to Nold (mean difference = 0.7, FDR-adjusted $p < 0.001$; Fig. 2A). Conversely, no significant group differences emerged for the IBF ($p = 0.9$, $\eta_p^2 = 0.0002$; Fig. 2B).

Regarding periodic features derived from the rsEEG power spectra, significant group effects were observed for aperiodic-corrected power at the IAF single-bin power peak ($p < 0.001$, $\eta_p^2 = 0.21$), within the rsEEG low-frequency alpha band ($p = 0.01$, $\eta_p^2 = 0.09$), and within the rsEEG high-frequency



alpha band ($p < 0.001$, $\eta_p^2 = 0.22$). Across all these measures, the ADCD group showed lower alpha-range power compared to the LBCD (IAF: FDR-adjusted $p = 0.03$; low-frequency alpha power: FDR-adjusted $p = 0.02$; high-frequency alpha power: FDR-adjusted $p = 0.04$) and the Nold group (IAF:

◂**Fig. 2** Estimated marginal means (dots) and 95% confidence intervals (bars) for periodic and aperiodic resting-state EEG (rsEEG) parameters in participants with cognitive decline due to Lewy body disease (LBCD), cognitive decline due to Alzheimer's disease (ADCD), and cognitively unimpaired older adults (Nold). **A** Individual alpha frequency (IAF, Hz); LBCD < ADCD < Nold (all FDR-adjusted *p*-values < 0.001). **B** Individual beta frequency (IBF, Hz); no significant group differences. **C** Aperiodic-corrected power at the IAF peak; LBCD > ADCD ($p < 0.05$, FDR-adjusted) and Nold > ADCD ($p < 0.001$). **D** Aperiodic-corrected power within the low-alpha band (IAF − 2 Hz to IAF); LBCD > ADCD ($p < 0.05$) and Nold > ADCD ($p < 0.05$). **E** Aperiodic-corrected power within the high-alpha band (IAF to IAF + 2 Hz); LBCD > ADCD ($p < 0.05$) and Nold > ADCD ($p < 0.001$). **F** Aperiodic-corrected power at the IBF peak; Nold > LBCD ($p < 0.001$) and Nold > ADCD ($p < 0.001$). **G** Delta residual power (1–3 Hz); no significant group differences. **H** Vigilance index (computed as the logarithm of the ratio between spectral power density at the IAF and IBF and spectral power density within the low-frequency range 1–5 Hz, with lower values indicating a relative shift toward slower-frequency activity and reduced quiet vigilance); LBCD < ADCD ($p < 0.05$, FDR-adjusted), LBCD < Nold ($p < 0.001$, FDR-adjusted), and ADCD < Nold ($p < 0.001$, FDR-adjusted). **I** Aperiodic exponent; LBCD > ADCD > Nold (all FDR-adjusted *p* -values < 0.001). **J** Aperiodic offset; LBCD > ADCD ($p < 0.001$) and LBCD > Nold ($p < 0.001$). EMM, estimated marginal mean; FDR, false discovery rate

FDR-adjusted $p < 0.001$; low-frequency alpha power: FDR-adjusted $p = 0.03$; high-frequency alpha power: FDR-adjusted $p < 0.001$; Fig. 2C–E). A significant effect was also found for the aperiodic-corrected rsEEG power at the IBF single-bin power peak ($p < 0.001$, $\eta_p^2 = 0.08$), with lower power in both LBCD and ADCD compared to Nold (FDR-adjusted $p < 0.001$; Fig. 2F). In contrast, no differences emerged in rsEEG delta residual power ($p = 0.4$, $\eta_p^2 = 0.02$; Fig. 2G), while significant group differences following a graded pattern were detected for the rsEEG vigilance index ($p < 0.01$, $\eta_p^2 = 0.28$). Specifically, the vigilance index was lower in the LBCD compared to the ADCD (FDR-adjusted $p = 0.01$) and the Nold group (FDR-adjusted $p < 0.001$), and in the ADCD group compared to the Nold group (FDR-adjusted $p < 0.001$; Fig. 2H). Topographic distributions and pairwise scalp difference maps of the vigilance index are illustrated in Fig. 3, highlighting widespread reductions in LBCD, particularly over posterior regions.

Concerning aperiodic rsEEG components, both the exponent and offset differed significantly across groups. For the aperiodic exponent ($p < 0.001$, $\eta_p^2 = 0.25$), values followed a LBCD > ADCD > Nold pattern, with all pairwise comparisons significant at FDR-adjusted $p < 0.001$ (Fig. 2I). For the aperiodic offset ($p < 0.001$, $\eta_p^2 = 0.11$), the LBCD group showed higher global values than both ADCD and Nold groups (FDR-adjusted $p < 0.001$), while ADCD and Nold did not differ significantly (Fig. 2J).

All significant effects observed at the whole-scalp level were replicated with comparable effect sizes in models restricted to the posterior scalp region (P7, P3, Pz, P4, P8, O1, and O2 electrodes), as reported in detail in Table S3 in the Supplementary Materials. Furthermore, electrode-level analyses also converged with these findings, mostly revealing spatially diffuse differences rather than sharply localized effects, aside from the expected central and posterior prominence in alpha- and beta-related periodic measures. The full set of scalp topographies and differential maps is presented in Supplementary Figures S1– S6.

Finally, in a supplementary sensitivity analysis addressing observed age differences between groups, the primary LMMs were repeated using an age-restricted Nold subsample ($N = 75$) with a closer age distribution to the clinical groups (mean age: 73.6 ± 5.5; no significant age effect in the one-way ANOVA with group as factor: $F = 1.2$, $p = 0.29$, $\eta_p^2 = 0.01$). As shown in Table S4 of the Supplementary Materials, results remained essentially unchanged, replicating the main effects for IAF, vigilance index, aperiodic exponent, and aperiodic offset, as well as the principal pairwise contrasts between groups.

Associations between rsEEG parameters and clinical outcomes in the LBCD group

Preliminarily, bivariate associations between clinical variables collected in the LBCD group (MMSE score, UPDRS-III score, and the binary-coded presence of visual hallucinations, cognitive fluctuations, and probable RBD) were examined. Partial correlations controlling for age, sex, and education are reported in Table S5 in the Supplementary Materials. MMSE scores showed small-to-moderate negative associations with both UPDRS-III ($rho = -0.21$, $p < 0.05$) scores and the presence of visual hallucinations ($r = -0.21$, $p < 0.05$). Cognitive fluctuations also correlated positively with visual hallucinations ($r = -0.27$, $p < 0.05$), reflecting the expected

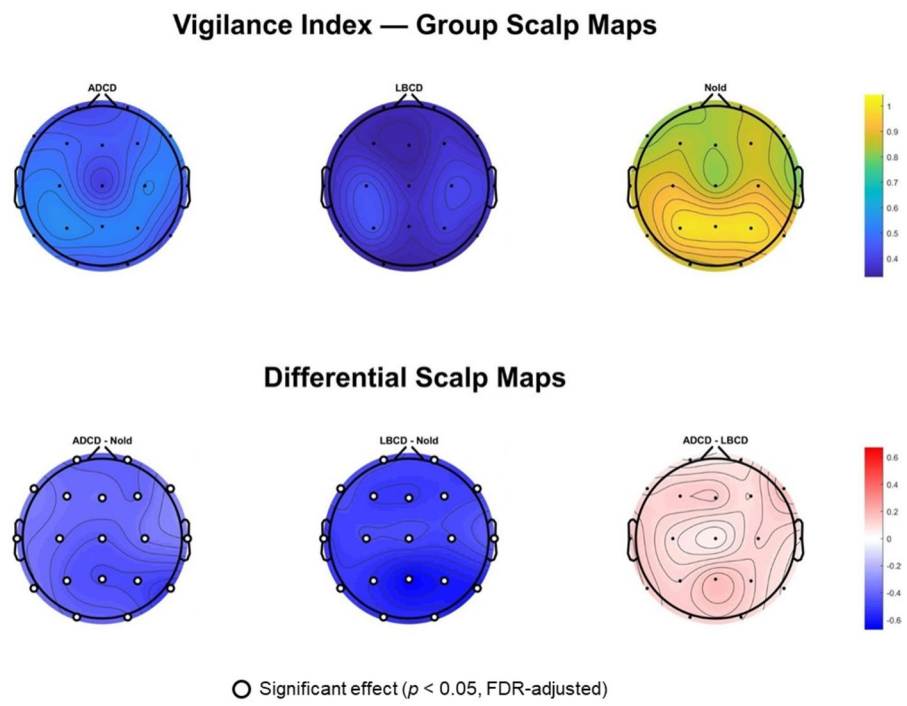


Fig. 3 The top row shows grand-average scalp maps of the resting-state EEG (rsEEG) vigilance index (computed as the logarithm of the ratio between spectral power density at the IAF and IBF and spectral power density within the low-frequency range 1–5 Hz) in participants with cognitive decline due to Alzheimer's disease (ADCD), cognitive decline due to Lewy body disease (LBCD), and cognitively unimpaired older adults (Nold). Warmer colors indicate higher values. The bottom row displays pairwise group differences (ADCD − Nold, LBCD − Nold, ADCD − LBCD) using a red-blue scale, where red indicates relatively higher values in the first group of each contrast and blue indicates relatively lower values. White circles denote electrodes showing significant between-group differences after false discovery rate (FDR) correction ($p < 0.05$). All models are adjusted for age, sex, and education. IAF, individual alpha frequency; IBF, individual beta frequency

clustering of neuropsychiatric manifestations in this population.

Subsequently, separate regression models were run to evaluate the associations between rsEEG variables that had shown significant group differences and the five clinical outcomes (i.e., MMSE, UPDRS-III, visual hallucinations, cognitive fluctuations, and RBD). For each outcome, five regression models were tested: covariates (age, sex, and education) were entered in a first block, and EEG predictors (summarized as global scalp averages) were entered in a second block. The EEG predictors were: rsEEG low- and high-frequency alpha aperiodic-corrected powers (as two predictors in a single model, to evaluate the full alpha range), aperiodic-corrected rsEEG power at the IBF, the vigilance index, the aperiodic exponent, and the aperiodic offset.

Among linear models predicting MMSE scores, the rsEEG alpha power model showed significant effects for both low- and high-frequency alpha band power ($\Delta R^2 = 0.09$ over the covariate-only model), with a negative association for rsEEG low-frequency alpha power ($p < 0.05$, $\beta = -0.28$) and a positive association for rsEEG high-frequency alpha power ($p < 0.01$, $\beta = 0.48$); significant positive associations with MMSE scores were also found for rsEEG IBF power ($p < 0.01$, $\beta = 0.26$; $\Delta R^2 = 0.06$ from the covariate-only model) and for the vigilance index ($p < 0.01$, $\beta = 0.31$; $\Delta R^2 = 0.06$ from the covariate-only model). No significant effects were observed for the aperiodic exponent or offset, and neither model improved explained variance beyond the covariate-only models.

For UPDRS-III scores (available for $N = 87$ LBCD participants), none of the rsEEG predictors reached significance (all $p > 0.4$), and final model R^2 values were low (ranging from 0.03 for the vigilance index to 0.043 for the aperiodic offset), indicating

no significant association between rsEEG and motor symptoms.

Logistic regression models predicting each binary-coded neuropsychiatric symptom (visual hallucinations, cognitive fluctuations, and probable RBD) were run on $N = 89$ participants with complete clinical data. No model predicting cognitive fluctuations or probable RBD reached significance. In contrast, the model including the rsEEG vigilance index as a predictor reached significance for visual hallucinations, with lower vigilance index values associated with a higher probability of visual hallucinations ($p = 0.002$; odds ratio = 0.21, 95% confidence interval 0.08–0.55). Figure 4 illustrates the adjusted scatterplots for significant linear associations, and Fig. 5 shows predicted probabilities of visual hallucinations across the observed values of the vigilance index. Coefficients and summary statistics for all significant models are reported in Table 2. Topographical patterns of vigilance index-related associations are shown in Fig. 6, indicating spatially diffuse relationships between lower vigilance index values, lower MMSE scores, and a higher likelihood of visual hallucinations.

Exploratory electrode-level analyses were also performed for all other clinical outcomes and all rsEEG predictors entered in the global regression models, as well as for aperiodic-corrected rsEEG power at the IAF peak. Overall, electrode-wise regression maps (Supplementary Figures S7– S11) were consistent with the results of the global models. Specifically, beyond the findings already reported for the vigilance index, significant widespread associations were observed between MMSE scores and aperiodic-corrected rsEEG IAF peak power and high-frequency rsEEG alpha power. No unanticipated effects or spatially distinct topographical patterns emerged.

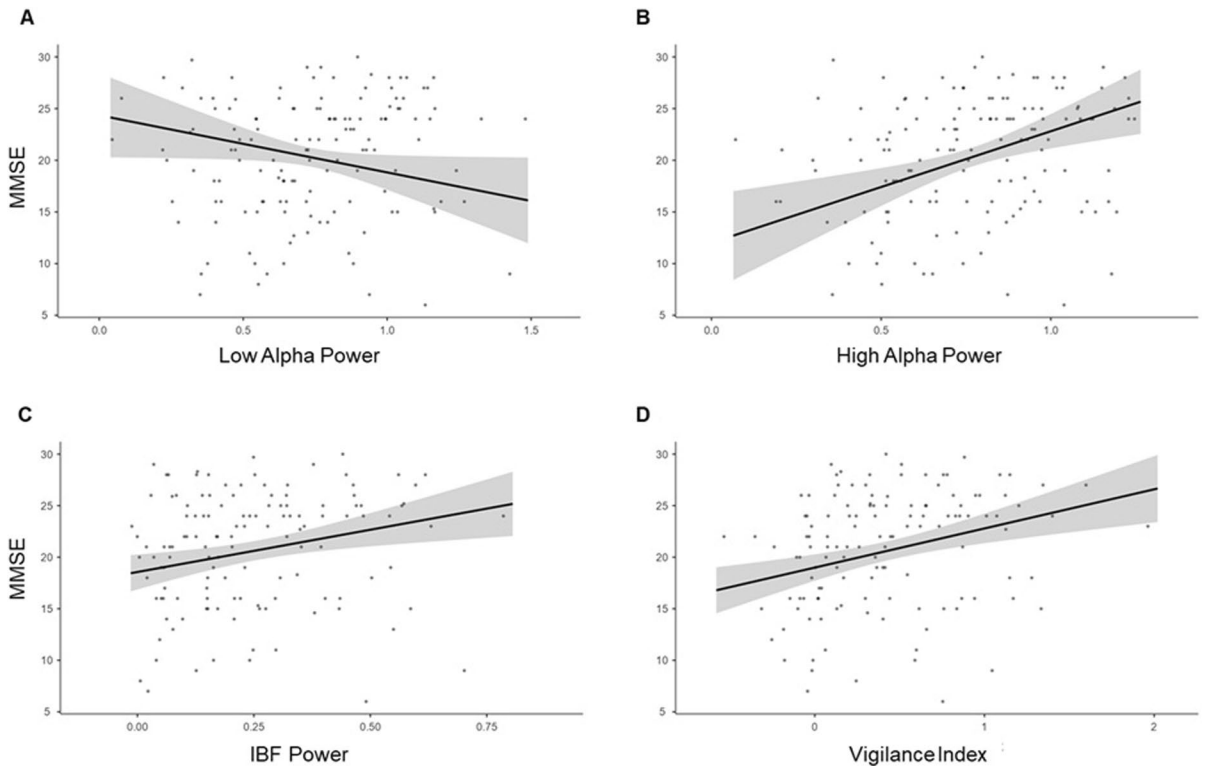


Fig. 4 Associations between global periodic resting-state EEG (rsEEG) measures and cognitive performance in participants with cognitive decline due to Lewy body disease (LBCD) ($N = 127$). Panels A–D show scatterplots with fitted regression lines and shaded 95% confidence intervals for the relationships between MMSE scores and **A** aperiodic-corrected power in the global low-alpha band, **B** aperiodic-corrected power in the global high-alpha band, **C** aperiodic-corrected power at the global individual beta frequency (IBF), and **D** the global vigilance index. IBF, individual beta frequency; MMSE, Mini-Mental State Examination

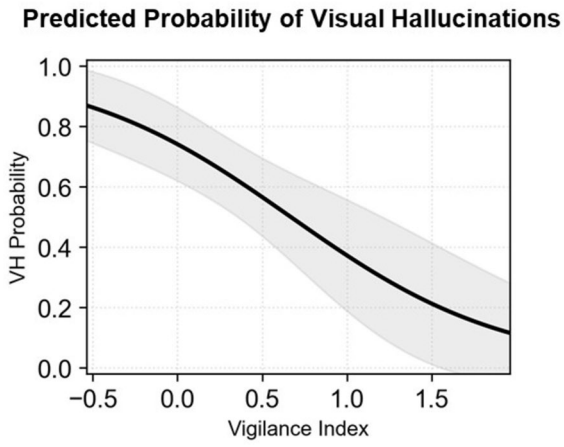


Fig. 5 Predicted probability of visual hallucinations as a function of the resting-state EEG (rsEEG) vigilance index in participants with cognitive decline due to Lewy body disease (LBCD) ($N = 89$). Predicted values are derived from the logistic regression model adjusting for age, sex, and education. The shaded band around the regression line represents the 95% confidence interval for the predicted probability. VH, visual hallucinations

Finally, to test the clinical specificity of the double-signed associations between MMSE and rsEEG alpha band power observed in the LBCD group (i.e., lower MMSE associated with higher low-alpha power, and higher MMSE associated with higher high-alpha power), the same regression model including both low- and high-frequency rsEEG alpha power as predictors was run separately in the ADCD and Nold groups. Supporting the specificity hypothesis, no significant associations were observed between MMSE and either low- or high-frequency rsEEG alpha power in the ADCD or Nold groups at $p < 0.05$.

Discussion

In this retrospective exploratory study based on the PDWAVES database (https://www.pdwaves.eu/), we examined the periodic and aperiodic components of rsEEG activity during quiet wakefulness in patients with LBCD ($N = 140$) and ADCD ($N = 135$) compared with cognitively unimpaired older adults (Nold; $N = 118$), while controlling for demographic characteristics and educational attainment. Both clinical groups were characterized by significant cognitive decline, with most participants in the mild-to-moderate dementia stage and the remainder classified as having MCI. By applying spectral parameterization [12, 31], we aimed to disentangle the neurophysiological mechanisms underlying the oscillatory (periodic) and broadband background (aperiodic exponent and offset) components of rsEEG power spectra in LBCD and ADCD. A further objective was to assess the clinical relevance of these markers specifically in LBCD by examining their associations with core disease manifestations, including cognitive deficits, motor impairment, visual hallucinations, cognitive fluctuations, and probable RBD.

Table 2 Summary of significant resting-state EEG (rsEEG) regression models in participants with cognitive decline due to Lewy body disease (LBCD). All models are adjusted for age, sex, and education. ΔR^2 refers to the increase in explained variance associated with adding the EEG predictor block

Model	EEG predictors	ΔR^2	Predictor	Estimate	SE	t/Z	p	β/OR (95% CI)
Linear models predicting MMSE								
Model 1 – Alpha bands ($N = 140$)	Low + High alpha power	0.09	Low alpha power	−5.5	2.7	−2.0	0.04	$\beta = -0.28$
			High alpha power	10.8	3.0	3.6	< 0.001	$\beta = 0.48$
Model 2 – Beta peak ($N = 129$)	IBF power	0.06	Beta peak power	8.2	2.7	3.0	0.003	$\beta = 0.26$
Model 3 – Vigilance index ($N = 129$)	Vigilance index	0.09	Vigilance index	3.8	1.0	3.8	< 0.001	$\beta = 0.31$
Logistic model predicting visual hallucinations								
Model 4 – Vigilance index ($N = 89$)	Vigilance index	–	Vigilance index	−1.6	0.5	−3.2	0.002	OR = 0.21 (95% CI 0.08–0.55)

CI confidence interval, *IBF* individual beta frequency, *OR* odds ratio

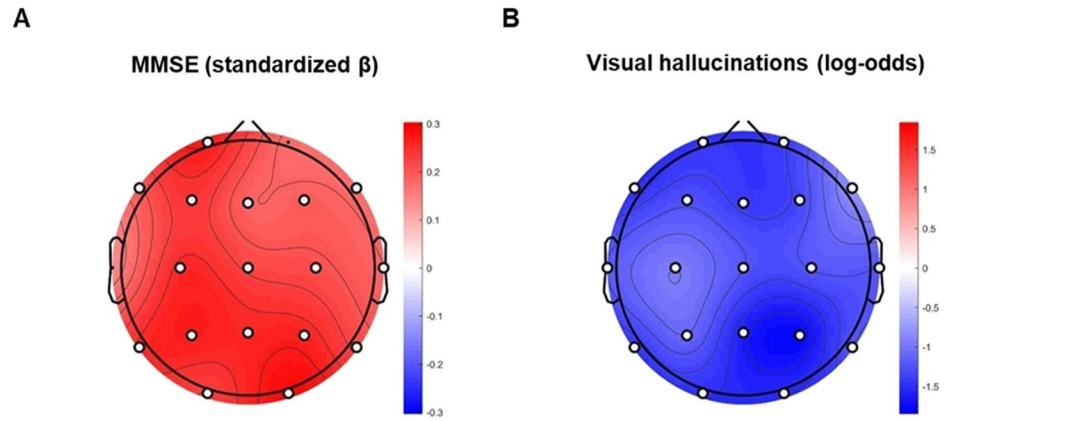


Fig. 6 Topographic maps show electrode-wise associations between the resting-state EEG (rsEEG) vigilance index (computed as the logarithm of the ratio between spectral power density at the IAF and IBF and spectral power density within the low-frequency range 1–5 Hz) and two clinical outcomes in participants with cognitive decline due to Lewy body disease (LBCD), controlling for age, sex, and education. **A** Standardized regression coefficients (β) from the linear model predicting Mini-Mental State Examination (MMSE) scores. Warmer colors indicate stronger positive associations (higher vigilance index associated with better cognitive performance), whereas cooler colors indicate weaker or negative associations. **B** Log-odds (regression coefficients) from the logistic model predicting the presence of visual hallucinations. Cooler colors indicate more negative associations (lower vigilance index associated with a higher probability of visual hallucinations). White circles mark electrodes with significant effects after false discovery rate (FDR) correction ($p < 0.05$). IAF, individual alpha frequency; IBF, individual beta frequency

Periodic and aperiodic spectral abnormalities in LBCD and ADCD

Compared with both Nold and ADCD participants, patients with LBCD showed a distinctive slowing of the periodic IAF peak, accompanied by lower periodic rsEEG alpha and beta power and higher spectral power in the slow-frequency theta range. These findings align with a reduced rsEEG vigilance index (defined as the ratio between aperiodic-corrected alpha–beta power and slow-frequency power), indicating impaired global cortical arousal during quiet wakefulness, with marked reductions widespread across the scalp (Figs. 2H and 3) and associations with lower MMSE scores and a higher probability of visual hallucinations (Figs. 4, 5, and 6). Moreover, LBCD patients also showed higher aperiodic exponent and offset values, suggesting stronger inhibitory cortical processes and reduced neuronal firing rates [18, 65].

Furthermore, lower periodic low-frequency alpha power (the so-called pre-alpha band; [5, 66, 67]) was associated with worse cognitive performance as measured by the MMSE, whereas higher high-frequency alpha power was associated with better MMSE scores. Consistently, a reduced periodic vigilance index was also related to the presence of visual hallucinations, supporting the notion that vigilance instability expressed through characteristic rsEEG rhythms contributes to the clinical phenotype of LBCD and its core neuropsychiatric manifestations.

Together, these results highlight substantial and spatially diffuse impairments in both oscillatory and non-oscillatory neurophysiological mechanisms regulating cortical arousal and vigilance in patients with LBCD, exceeding those observed in patients with ADCD. At the same time, reduced periodic beta power emerged as a reliable differentiating feature in both LBCD and ADCD relative to Nold participants, consistent with the well-documented global slowing of rsEEG activity in neurodegenerative conditions [7, 68–70].

Generally, the present results extend earlier EEG findings reporting a slower IAF peak (≤ 8 Hz) and elevated power in delta, theta, and pre-alpha ranges in LBCD compared with ADCD and Nold participants

[5, 6, 9, 10, 66, 67]. They also align with studies showing increased posterior pre-alpha/theta activity and stronger theta rhythms in LBCD linked to cognitive decline and visual hallucinations [70, 71], as well as with recent evidence of elevated aperiodic exponent and offset in synucleinopathies with cognitive impairment (i.e., LBCD and PDCD) relative to ADCD and Nold groups [24, 25, 27, 29].

Frequency slowing of the periodic IAF peak likely reflects disrupted thalamocortical and corticothalamic circuitry supporting alpha-band synchrony (8–10 Hz), which is critical for sustaining sensory readiness, attentional control, and quiet wakefulness [7, 14–16]. In parallel, an increased aperiodic exponent may indicate reduced excitation or heightened inhibition across large-scale neuronal populations, whereas a higher offset may reflect lower neuronal firing rates and synaptic input strength [18–21]. Supporting these conclusions, rsEEG–fMRI studies show that alpha modulation reflects attentional network functioning, while the aperiodic component correlates with slow metabolic fluctuations [15, 16, 72, 73]. Nevertheless, interpretations of aperiodic markers should remain cautious, as their physiological basis is not yet fully understood [17, 19, 65], and they may be influenced by residual artifacts (ocular and/or muscular), reference schemes, volume conduction, nonlinear neural–glial interactions, or membrane time constants [65, 74–78].

Overall, patients with LBCD appear to manifest a neurophysiological state of mixed wakefulness and drowsiness, marked by heightened cortical inhibitory tone and reduced arousal, in line with the thalamocortical dysrhythmia hypothesis [79, 80]. According to this model, reduced excitatory input to thalamocortical neurons induces low-frequency bursting (< 7 Hz), impairing cortical relay functions and vigilance regulation in a transition toward light sleep. In LBCD, abnormal cholinergic signaling from the pedunculopontine nucleus and basal forebrain [81, 82] may further promote theta-burst firing in higher-order thalamic nuclei, ultimately contributing to vigilance dysfunctions and sensory hallucinations [83, 84].

Methodological remarks

This study examined periodic and aperiodic rsEEG spectra in a multicenter cohort of LBCD, ADCD, and Nold participants. Although sample sizes were relatively large, the number of LBCD and ADCD participants with MCI was limited, preventing subgroup analyses based on the degree of cognitive decline. Regarding the rsEEG analysis, the 19-channel montage may not have provided sufficient spatial resolution to fully capture localized topographical patterns. In addition, the Nold control group was younger on average than the two clinical groups. Although age was systematically included as a covariate in all inferential models, and statistical adjustment was deliberately preferred over strict matching procedures in order to retain the full multicenter sample and avoid additional selection biases related to participant exclusion, residual age-related confounding cannot be entirely ruled out. However, supplementary sensitivity analyses based on an age-restricted Nold subsample yielded results closely comparable to the primary models, suggesting that the main findings were not solely explained by age differences between groups. At the same time, other potentially relevant demographic and clinical confounders (e.g., cardiovascular risk factors or socioeconomic variables) were not systematically accounted for. Moreover, although participants taking regular medication were asked to delay administration until after the EEG session in order to reduce acute pharmacological effects, the relative contributions of neuropathological burden and chronic pharmacological treatments to periodic and aperiodic rsEEG spectral alterations could not be completely determined in this naturalistic, multicenter sample. In particular, residual influences of chronic treatments on rsEEG spectral measures [27, 85–88] cannot be fully excluded, especially in the LBCD group, where the use of dopaminergic, cholinergic, and psychotropic medications was relatively frequent (Supplementary Table S1). Future research should rely on larger, heterogeneous, longitudinal LBCD and ADCD cohorts with multimodal assessments of brain activity and ongoing sleep–wake rhythms (e.g., EEG, MRI/PET, and actigraphy), with a particular focus on the neuromodulatory subcortical systems implicated in vigilance regulation.

Conclusions

This exploratory study evaluated periodic and aperiodic rsEEG spectral differences in a large multicenter cohort of participants with LBCD, ADCD, and Nold

individuals. By decomposing rsEEG power spectra into oscillatory peaks and aperiodic background activity, we sought to clarify the neurophysiological mechanisms contributing to rsEEG slowing in LBCD and ADCD, and to examine the clinical correlates of these markers in LBCD, with a particular focus on symptoms and manifestations linked to vigilance regulation.

Patients with LBCD were characterized by marked slowing of the periodic IAF peak and a reduced vigilance index, reflecting lower periodic alpha and beta power together with increased slow-frequency activity. Within the LBCD group, lower periodic low-frequency alpha power was associated with poorer cognitive performance, whereas higher high-frequency alpha power predicted better cognition. Furthermore, a reduced vigilance index was also associated with the presence of visual hallucinations, while increased aperiodic exponent and offset values in LBCD suggested stronger inhibitory cortical processes and reduced neuronal firing.

Building on these findings, future studies should investigate whether these EEG measures reflecting vigilance dysfunction could serve as clinically informative biomarkers to guide targeted, vigilance-focused interventions, including non-pharmacological strategies such as electromagnetic or audiovisual stimulation (e.g., 40 Hz multisensory stimulation) acting directly on rsEEG brain rhythms.

Authors' contribution CB and MC designed the study. APA, MDB, MC, SL, BB, CDP, GN, VHI, and LB pre-processed and analyzed the EEG data. MC, SL, and APA performed periodic and aperiodic EEG spectral analyses. MC and CDP performed the statistical analyses. CB supervised the data analysis process. MC and RL drafted the manuscript. CB proofread and edited the manuscript, collected the data, participated in editing the manuscript, and discussing the results.

Funding Open access funding provided by Università degli Studi di Roma La Sapienza within the CRUI-CARE Agreement. The present study was developed based on the data of the PDWAVES Consortium (https://www.pdwaves.eu/) and the PharmaCog project. The electroencephalographic data recording and analysis were partially supported by the funds of "Ricerca Corrente" attributed by the Italian Ministry of Health to the IRCCS Synlab SDN of Naples (Italy), Oasi Research Institute-IRCCS, Troina (Italy), IRCCS Istituto Centro San Giovanni di Dio Fatebenefratelli (Italy), IRCCS Ospedale Policlinico San Martino, Genova (Italy), IRCCS, San Camillo Hospital, Venice (Italy), and IRCCS San Raffaele of Rome (Italy).

Matteo Carpi's research activities in the Open SIESTA Lab of Sapienza University of Rome were supported by the grants with the following references: Progetto ECS 0000024 "Rome Technopole", CUP B83C22002820006, PNRR Mission 4 Component 2 Investment 1.5; CUP B53C23002080006, PNRR Mission 4 Component 1 ("Borse dottorati generici ricerca PNRR"). Both grants were funded by the European Union's NextGenerationEU program through the Italian Ministry of University.

Claudio Babiloni was partially supported by a HORIZON 2021 project grant titled "eBRAIN-Health – Actionable Multilevel Health Data", Call and Sponsor: HORIZON 2021, HORIZON-INFRA-2021-TECH-01 (HORIZON-INFRA-2021-TECH-01–01 – Interdisciplinary digital twins for modeling and simulating complex phenomena at the service of research infrastructure communities), Grant Agreement: GAP-101058516.

Claudio Del Percio was partially supported by a grant from the Italian Ministry of University for the project titled "Amyloid-related cortical excitability in patients with MCI due to Alzheimer's disease", Call and Sponsor: ANNUAL STRATEGIC PROGRAM OF ITALIAN MINISTRY OF UNIVERSITY AND SCIENTIFIC AND TECHNOLOGICAL RESEARCH, Grant Agreement: 2022FJAXY8.

Matteo Pardini was supported by a grant from the Italian Ministry of University with the code PE00000006 "PNRR MUR Investment 1.5 (M4C2)" for the project "A multiscale integrated approach to the study of the nervous system in health and disease (MNESYS)".

Paolo Barone and Angelo Antonini were partially supported by a grant from the Italian Ministry of Health for the project titled "Effects of endogenous and exogenous risk factors in patients with Alzheimer's and Parkinson's diseases using clinical indexes and endophenotypes (biomarkers) as inputs to artificial intelligence (PREDICT-NEURODEGEN)". Call and Sponsor: ANNUAL STRATEGIC PROGRAM OF ITALIAN MINISTRY OF HEALTH, Grant Agreement: PNRR-MAD-2022–12376415.

Marianna Amboni and Fabrizio Stocchi were partially supported by a grant from the Italian Ministry of Health for the project titled "Specific diagnostic biomarker profiles of different clinical clusters in DLB (DLB-cluster)". Call and Sponsor: ANNUAL STRATEGIC PROGRAM OF ITALIAN MINISTRY OF HEALTH, Grant Agreement: PNRR-MCNT2-2023–12377423.

Laura Bonanni was partially supported by a grant from the Italian Ministry of University for the project titled "Assessment of brain functions in Lewy Body disease patients using telemonitoring Digital markers as inputs to artificial intelligence (LBDigital)". Call and Sponsor: ANNUAL STRATEGIC PROGRAM OF THE ITALIAN MINISTRY OF UNIVERSITY AND SCIENTIFIC AND TECHNOLOGICAL RESEARCH, Grant Agreement: 2010SH7H3F.

Raffaele Ferri was partially supported by a grant from the Italian Ministry of Health for the project titled "Integrating sleep–wake oscillatory activities and liquid biopsy as innovative biomarkers for multimodal diagnosis in preclinical and prodromal Alzheimer's disease (ISLA)". Call and Sponsor: ANNUAL STRATEGIC PROGRAM OF THE ITALIAN MINISTRY OF HEALTH, Grant Agreement: PNRR-MCNT2-2023–12377357.

John Paul Taylor was supported by the Newcastle NIHR Biomedical Research Centre.

Data availability The datasets analyzed during the current study are not publicly available due to privacy considerations. De-identified data can be made available from the corresponding author upon reasonable request.

Declarations

Ethics and consent to participate The study was conducted in accordance with the Declaration of Helsinki and with local regulations governing research involving human participants. The study protocol was approved by the institutional ethics committees of all participating centers within the PDWAVES Consortium. Written informed consent was obtained from all participants prior to inclusion in the study.

Competing interest The authors declare no competing interests.

Open Access This article is licensed under a Creative Commons Attribution 4.0 International License, which permits use, sharing, adaptation, distribution and reproduction in any medium or format, as long as you give appropriate credit to the original author(s) and the source, provide a link to the Creative Commons licence, and indicate if changes were made. The images or other third party material in this article are included in the article's Creative Commons licence, unless indicated otherwise in a credit line to the material. If material is not included in the article's Creative Commons licence and your intended use is not permitted by statutory regulation or exceeds the permitted use, you will need to obtain permission directly from the copyright holder. To view a copy of this licence, visit http://creativecommons.org/licenses/by/4.0/.

References

1. Arvanitakis Z, Shah RC, Bennett DA. Diagnosis and management of dementia: review. JAMA. 2019;322:1589. https://doi.org/10.1001/jama.2019.4782.
2. Mueller C, Ballard C, Corbett A, Aarsland D. The prognosis of dementia with Lewy bodies. Lancet Neurol. 2017;16:390–8. https://doi.org/10.1016/S1474-4422(17)30074-1.
3. Jack CR, Andrews JS, Beach TG, Buracchio T, Dunn B, Graf A, et al. Revised criteria for diagnosis and staging of Alzheimer's disease: Alzheimer's Association Workgroup. Alzheimers Dement. 2024;20:5143–69. https://doi.org/10.1002/alz.13859.
4. Jack CR, Bennett DA, Blennow K, Carrillo MC, Dunn B, Haeberlein SB, et al. NIA-AA Research framework: toward a biological definition of Alzheimer's disease. Alzheimers Dement J Alzheimers Assoc. 2018;14:535–62. https://doi.org/10.1016/j.jalz.2018.02.018.
5. McKeith IG, Boeve BF, Dickson DW, Halliday G, Taylor J-P, Weintraub D, et al. Diagnosis and management of dementia with Lewy bodies: fourth consensus report of the DLB Consortium. Neurology. 2017;89:88–100. https://doi.org/10.1212/WNL.0000000000004058.
6. McKeith IG, Ferman TJ, Thomas AJ, Blanc F, Boeve BF, Fujishiro H, et al. Research criteria for the diagnosis of prodromal dementia with Lewy bodies. Neurology. 2020;94:743–55. https://doi.org/10.1212/WNL.0000000000009323.
7. Babiloni C, Blinowska K, Bonanni L, Cichocki A, De Haan W, Del Percio C, et al. What electrophysiology tells us about Alzheimer's disease: a window into the synchronization and connectivity of brain neurons. Neurobiol Aging. 2020;85:58–73. https://doi.org/10.1016/j.neurobiolaging.2019.09.008.
8. Babiloni C. The dark side of Alzheimer's disease: neglected physiological biomarkers of brain hyperexcitability and abnormal consciousness level. J Alzheimers Dis JAD. 2022;88:801–7. https://doi.org/10.3233/JAD-220582.
9. Babiloni C, Del Percio C, Lizio R, Noce G, Lopez S, Soricelli A, et al. Abnormalities of resting-state functional cortical connectivity in patients with dementia due to Alzheimer's and Lewy body diseases: an EEG study. Neurobiol Aging. 2018;65:18–40. https://doi.org/10.1016/j.neurobiolaging.2017.12.023.
10. Mahajan A, Jaramillo-Jimenez A, D'Anselmo A, Prete G, Bristot L, Varanese S, et al. Quantitative electroencephalography in the diagnosis of dementia with Lewy bodies. Clin Neurophysiol Pract. 2025;10:222–33. https://doi.org/10.1016/j.cnp.2025.06.008.
11. Rossini PM, Di Iorio R, Vecchio F, Anfossi M, Babiloni C, Bozzali M, et al. Early diagnosis of Alzheimer's disease: the role of biomarkers including advanced EEG signal analysis. Report from the IFCN-sponsored panel of experts. Clin Neurophysiol. 2020;131:1287–310. https://doi.org/10.1016/j.clinph.2020.03.003.
12. Donoghue T, Haller M, Peterson EJ, Varma P, Sebastian P, Gao R, et al. Parameterizing neural power spectra into periodic and aperiodic components. Nat Neurosci. 2020;23:1655–65. https://doi.org/10.1038/s41593-020-00744-x.
13. Voytek B, Kramer MA, Case J, Lepage KQ, Tempesta ZR, Knight RT, et al. Age-related changes in 1/f neural electrophysiological noise. J Neurosci Off J Soc Neurosci. 2015;35:13257–65. https://doi.org/10.1523/JNEUROSCI.2332-14.2015.
14. Babiloni C, Lopez S, Noce G, Ferri R, Panerai S, Catania V, et al. Relationship between default mode network and resting-state electroencephalographic alpha rhythms in cognitively unimpaired seniors and patients with dementia due to Alzheimer's disease. Cereb Cortex. 2023;33:10514–27. https://doi.org/10.1093/cercor/bhad300.
15. Jacob MS, Roach BJ, Sargent KS, Mathalon DH, Ford JM. Aperiodic measures of neural excitability are associated with anticorrelated hemodynamic networks at rest: a combined EEG-fMRI study. Neuroimage. 2021;245:118705. https://doi.org/10.1016/j.neuroimage.2021.118705.
16. Wen H, Liu Z. Broadband electrophysiological dynamics contribute to global resting-state fMRI signal. J Neurosci

Off J Soc Neurosci. 2016;36:6030–40. https://doi.org/10.1523/JNEUROSCI.0187-16.2016.
17. Donoghue T. A systematic review of aperiodic neural activity in clinical investigations. Eur J Neurosci. 2025;62:e70255. https://doi.org/10.1111/ejn.70255.
18. Gao R, Peterson EJ, Voytek B. Inferring synaptic excitation/inhibition balance from field potentials. Neuroimage. 2017;158:70–8. https://doi.org/10.1016/j.neuroimage.2017.06.078.
19. Lombardi F, Herrmann HJ, De Arcangelis L. Balance of excitation and inhibition determines 1/f power spectrum in neuronal networks. Chaos. 2017;27:047402. https://doi.org/10.1063/1.4979043.
20. Manning JR, Jacobs J, Fried I, Kahana MJ. Broadband shifts in local field potential power spectra are correlated with single-neuron spiking in humans. J Neurosci Off J Soc Neurosci. 2009;29:13613–20. https://doi.org/10.1523/JNEUROSCI.2041-09.2009.
21. Winawer J, Kay KN, Foster BL, Rauschecker AM, Parvizi J, Wandell BA. Asynchronous broadband signals are the principal source of the BOLD response in human visual cortex. Curr Biol. 2013;23:1145–53. https://doi.org/10.1016/j.cub.2013.05.001.
22. Wen H, Liu Z. Separating Fractal and oscillatory components in the power spectrum of neurophysiological signal. Brain Topogr. 2016;29:13–26. https://doi.org/10.1007/s10548-015-0448-0.
23. Azami H, Zrenner C, Brooks H, Zomorrodi R, Blumberger DM, Fischer CE, et al. Beta to theta power ratio in EEG periodic components as a potential biomarker in mild cognitive impairment and Alzheimer's dementia. Alzheimers Res Ther. 2023;15:133. https://doi.org/10.1186/s13195-023-01280-z.
24. Burelo M, Bray J, Gulka O, Firbank M, Taylor J-P, Platt B. Advanced qEEG analyses discriminate between dementia subtypes. J Neurosci Methods. 2024;409:110195. https://doi.org/10.1016/j.jneumeth.2024.110195.
25. Jaramillo-Jimenez A, Mantilla-Ramos Y-J, Tovar-Rios DA, Lopera F, Aguillón D, Ochoa-Gomez JF, et al. Characterizing resting-state EEG oscillatory and aperiodic activity in neurodegenerative diseases: a multicentric study. Comput Biol Med. 2025;197:111080. https://doi.org/10.1016/j.compbiomed.2025.111080.
26. Kopčanová M, Tait L, Donoghue T, Stothart G, Smith L, Flores-Sandoval AA, et al. Resting-state EEG signatures of Alzheimer's disease are driven by periodic but not aperiodic changes. Neurobiol Dis. 2024;190:106380. https://doi.org/10.1016/j.nbd.2023.106380.
27. McKeown DJ, Jones M, Pihl C, Finley AJ, Kelley N, Baumann O, et al. Medication-invariant resting aperiodic and periodic neural activity in Parkinson's disease. Psychophysiology. 2024;61:e14478. https://doi.org/10.1111/psyp.14478.
28. Merkin A, Sghirripa S, Graetz L, Smith AE, Hordacre B, Harris R, et al. Do age-related differences in aperiodic neural activity explain differences in resting EEG alpha? Neurobiol Aging. 2023;121:78–87. https://doi.org/10.1016/j.neurobiolaging.2022.09.003.
29. Rosenblum Y, Shiner T, Bregman N, Giladi N, Maidan I, Fahoum F, et al. Decreased aperiodic neural activity in Parkinson's disease and dementia with Lewy bodies. J Neurol. 2023;270:3958–69. https://doi.org/10.1007/s00415-023-11728-9.
30. Wang Z, Liu A, Yu J, Wang P, Bi Y, Xue S, et al. The effect of aperiodic components in distinguishing Alzheimer's disease from frontotemporal dementia. GeroScience. 2023;46:751–68. https://doi.org/10.1007/s11357-023-01041-8.
31. McKeown DJ, Finley AJ, Kelley NJ, Cavanagh JF, Keage HAD, Baumann O, et al. Test-retest reliability of spectral parameterization by 1/f characterization using SpecParam. Cereb Cortex. 2024;34(1):bhad482. https://doi.org/10.1093/cercor/bhad482.
32. Popov T, Tröndle M, Baranczuk-Turska Z, Pfeiffer C, Haufe S, Langer N. Test–retest reliability of resting-state EEG in young and older adults. Psychophysiology. 2023;60:e14268. https://doi.org/10.1111/psyp.14268.
33. Faul F, Erdfelder E, Lang A-G, Buchner A. G*Power 3: a flexible statistical power analysis program for the social, behavioral, and biomedical sciences. Behav Res Methods. 2007;39:175–91. https://doi.org/10.3758/bf03193146.
34. Cummings JL, Mega M, Gray K, Rosenberg-Thompson S, Carusi DA, Gornbein J. The neuropsychiatric inventory: comprehensive assessment of psychopathology in dementia. Neurology. 1994;44:2308–14. https://doi.org/10.1212/wnl.44.12.2308.
35. Walker MP, Ayre GA, Cummings JL, Wesnes K, McKeith IG, O'Brien JT, et al. The clinician assessment of fluctuation and the one day fluctuation assessment scale: two methods to assess fluctuating confusion in dementia. Br J Psychiatry. 2000;177:252–6. https://doi.org/10.1192/bjp.177.3.252.
36. American Academy of Sleep Medicine. International Classification of Sleep Disorders. 3rd ed. Darien, IL: American Academy of Sleep Medicine; 2014.
37. Goetz CG, Tilley BC, Shaftman SR, Stebbins GT, Fahn S, Martinez-Martin P, et al. Movement disorder society-sponsored revision of the unified Parkinson's disease rating scale (MDS-UPDRS): scale presentation and clinimetric testing results. Mov Disord. 2008;23:2129–70. https://doi.org/10.1002/mds.22340.
38. American Psychiatric Association. Diagnostic and Statistical Manual of Mental Disorders. 5th ed. Arlington, VA: Author; 2013.
39. McKhann G, Drachman D, Folstein M, Katzman R, Price D, Stadlan EM. Clinical diagnosis of Alzheimer's disease: report of the NINCDS-ADRDA Work Group* under the auspices of Department of Health and Human Services Task Force on Alzheimer's Disease. Neurology. 1984;34:939–939. https://doi.org/10.1212/WNL.34.7.939.
40. Folstein MF, Folstein SE, McHugh PR. "Mini-mental state". A practical method for grading the cognitive state of patients for the clinician. J Psychiatr Res. 1975;12:189–98. https://doi.org/10.1016/0022-3956(75)90026-6.
41. Babiloni C, Barry RJ, Başar E, Blinowska KJ, Cichocki A, Drinkenburg WHIM, et al. International Federation of Clinical Neurophysiology (IFCN) - EEG research workgroup: recommendations on frequency and topographic analysis of resting state EEG rhythms. Part 1:

applications in clinical research studies. Clin Neurophysiol. 2020;131:285–307. https://doi.org/10.1016/j.clinph.2019.06.234.
42. Babiloni C, Jakhar D, Tucci F, Del Percio C, Lopez S, Soricelli A, et al. Resting state electroencephalographic alpha rhythms are sensitive to Alzheimer's disease mild cognitive impairment progression at a 6-month follow-up. Neurobiol Aging. 2024;137:19–37. https://doi.org/10.1016/j.neurobiolaging.2024.01.013.
43. Babiloni C, Noce G, Tucci F, Jakhar D, Ferri R, Panerai S, et al. Poor reactivity of posterior electroencephalographic alpha rhythms during the eyes open condition in patients with dementia due to Parkinson's disease. Neurobiol Aging. 2024;135:1–14. https://doi.org/10.1016/j.neurobiolaging.2023.11.010.
44. Delorme A, Makeig S. EEGLAB: an open source toolbox for analysis of single-trial EEG dynamics including independent component analysis. J Neurosci Methods. 2004;134:9–21. https://doi.org/10.1016/j.jneumeth.2003.10.009.
45. Crespo-Garcia M, Atienza M, Cantero JL. Muscle artifact removal from human sleep EEG by using independent component analysis. Ann Biomed Eng. 2008;36:467–75. https://doi.org/10.1007/s10439-008-9442-y.
46. Jung TP, Makeig S, Humphries C, Lee TW, McKeown MJ, Iragui V, et al. Removing electroencephalographic artifacts by blind source separation. Psychophysiology. 2000;37:163–78.
47. Niedermeyer E. Alpha rhythms as physiological and abnormal phenomena. Int J Psychophysiol. 1997;26:31–49. https://doi.org/10.1016/S0167-8760(97)00754-X.
48. Pfurtscheller G, Lopes da Silva FH. Event-related EEG/MEG synchronization and desynchronization: basic principles. Clin Neurophysiol Off J Int Fed Clin Neurophysiol. 1999;110:1842–57. https://doi.org/10.1016/s1388-2457(99)00141-8.
49. Klimesch W. EEG alpha and theta oscillations reflect cognitive and memory performance: a review and analysis. Brain Res Brain Res Rev. 1999;29:169–95. https://doi.org/10.1016/s0165-0173(98)00056-3.
50. Olbrich S, Mulert C, Karch S, Trenner M, Leicht G, Pogarell O, et al. EEG-vigilance and BOLD effect during simultaneous EEG/fMRI measurement. Neuroimage. 2009;1;45(2):319–32.
51. Liu TT, Falahpour M. Vigilance effects in resting-state fMRI. Front Neurosci. 2020;14:321. https://doi.org/10.3389/fnins.2020.00321.
52. Carpi M, Henao Isaza V, Noce G, Salamone EM, Del Percio C, Lopez S, et al. Periodic and aperiodic electroencephalographic rhythms during vigilance transitions in Alzheimer's disease mild cognitive impairment. Ann N Y Acad Sci. 2026;1555:e70194. https://doi.org/10.1111/nyas.70194.
53. Hori T, Hayashi M, Morikawa T. Topographical EEG changes and the hypnagogic experience. In: Ogilvie RD, Harsh JR, editors. Sleep onset: Normal and abnormal processes. Washington: Am Psychol Assoc; 1994. p. 237–53.https://content.apa.org/books/10166-014.
54. Ogilvie RD. The process of falling asleep. Sleep Med Rev. 2001;5:247–70. https://doi.org/10.1053/smrv.2001.0145.
55. Lacaux C, Strauss M, Bekinschtein TA, Oudiette D. Embracing sleep-onset complexity. Trends Neurosci. 2024;47:273–88. https://doi.org/10.1016/j.tins.2024.02.002.
56. Hertig-Godeschalk A, Skorucak J, Malafeev A, Achermann P, Mathis J, Schreier DR. Microsleep episodes in the borderland between wakefulness and sleep. Sleep. 2019;zsz163.https://doi.org/10.1093/sleep/zsz163.
57. The jamovi project. jamovi (Version 2.5) [Internet]. 2024.https://www.jamovi.org/.
58. Gallucci M. GAMLj: General analyses for linear models [Internet]. 2019. https://gamlj.github.io/.
59. R Core Team. R: a language and environment for statistical computing. Vienna, Austria: R Foundation for Statistical Computing; 2024.
60. Benjamini Y, Hochberg Y. Controlling the false discovery rate: a practical and powerful approach to multiple testing. J R Stat Soc Ser B Methodol. 1995;57:289–300. https://doi.org/10.1111/j.2517-6161.1995.tb02031.x.
61. Del Percio C, Lizio R, Lopez S, Noce G, Jakhar D, Carpi M, et al. Resting-state electroencephalographic rhythms depend on sex in patients with dementia due to Parkinson's and Lewy body diseases: an exploratory study. Neurobiol Dis. 2025;206:106807. https://doi.org/10.1016/j.nbd.2025.106807.
62. Lopez S, Del Percio C, Lizio R, Noce G, Jakhar D, Soricelli A, et al. The compensatory effect of education as revealed by resting-state electroencephalographic alpha rhythms in patients with dementia due to Parkinson's disease: findings from an exploratory study. GeroScience. 2026;48:1189–218. https://doi.org/10.1007/s11357-025-01703-9.
63. Hair JF, editor. Multivariate data analysis: a global perspective. 7. ed., global ed. Upper Saddle River, NJ Munich: Pearson; 2010.
64. Tabachnick BG, Fidell LS. Using multivariate statistics. Pearson new international edition, sixth edition. Harlow: Pearson; 2014.
65. Brake N, Duc F, Rokos A, Arseneau F, Shahiri S, Khadra A, et al. A neurophysiological basis for aperiodic EEG and the background spectral trend. Nat Commun. 2024;15:1514. https://doi.org/10.1038/s41467-024-45922-8.
66. Bonanni L, Franciotti R, Nobili F, Kramberger MG, Taylor J-P, Garcia-Ptacek S, et al. EEG markers of dementia with Lewy bodies: a multicenter cohort study. J Alzheimers Dis. 2016;54:1649–57. https://doi.org/10.3233/JAD-160435.
67. Bonanni L, Thomas A, Tiraboschi P, Perfetti B, Varanese S, Onofrj M. EEG comparisons in early Alzheimer's disease, dementia with Lewy bodies and Parkinson's disease with dementia patients with a 2-year follow-up. Brain. 2008;131:690–705. https://doi.org/10.1093/brain/awm322.
68. Jeong J. EEG dynamics in patients with Alzheimer's disease. Clin Neurophysiol. 2004;115:1490–505. https://doi.org/10.1016/j.clinph.2004.01.001.
69. Meghdadi AH, Stevanović Karić M, McConnell M, Rupp G, Richard C, Hamilton J, et al. Resting state EEG biomarkers of cognitive decline associated with

Alzheimer's disease and mild cognitive impairment. PLoS ONE. 2021;16:e0244180. https://doi.org/10.1371/journal.pone.0244180.
70. Schumacher J, Taylor J-P, Hamilton CA, Firbank M, Cromarty RA, Donaghy PC, et al. Quantitative EEG as a biomarker in mild cognitive impairment with Lewy bodies. Alzheimers Res Ther. 2020;12:82. https://doi.org/10.1186/s13195-020-00650-1.
71. Onofrj M, Espay AJ, Bonanni L, Delli Pizzi S, Sensi SL. Hallucinations, somatic-functional disorders of PD-DLB as expressions of thalamic dysfunction. Mov Disord. 2019;34:1100–11. https://doi.org/10.1002/mds.27781.
72. Colombo MA, Napolitani M, Boly M, Gosseries O, Casarotto S, Rosanova M, et al. The spectral exponent of the resting EEG indexes the presence of consciousness during unresponsiveness induced by propofol, xenon, and ketamine. Neuroimage. 2019;189:631–44. https://doi.org/10.1016/j.neuroimage.2019.01.024.
73. Østergaard FG, Penninx BWJH, Das N, Arango C, van der Wee N, Winter-van Rossum I, et al. The aperiodic exponent of neural activity varies with vigilance state in mice and men. PLoS ONE. 2024;19:e0301406. https://doi.org/10.1371/journal.pone.0301406.
74. Gerster M, Waterstraat G, Litvak V, Lehnertz K, Schnitzler A, Florin E, et al. Separating neural oscillations from aperiodic 1/f activity: challenges and recommendations. Neuroinformatics. 2022;20:991–1012. https://doi.org/10.1007/s12021-022-09581-8.
75. Kozhemiako N, Mylonas D, Pan JQ, Prerau MJ, Redline S, Purcell SM. Sources of variation in the spectral slope of the sleep EEG. eNeuro. 2022;9:ENEURO.0094-22.2022. https://doi.org/10.1523/ENEURO.0094-22.2022.
76. Salvatore SV, Lambert PM, Benz A, Rensing NR, Wong M, Zorumski CF, et al. Periodic and aperiodic changes to cortical EEG in response to pharmacological manipulation. J Neurophysiol. 2024;131:529–40. https://doi.org/10.1152/jn.00445.2023.
77. Schmidt F, Danböck SK, Trinka E, Klein DP, Demarchi G, Weisz N. Age-related changes in 'cortical' 1/f dynamics are linked to cardiac activity. Elife. 2025;13:RP100605. https://doi.org/10.7554/eLife.100605.3.
78. Untiet V, Beinlich FRM, Kusk P, Kang N, Ladrón-de-Guevara A, Song W, et al. Astrocytic chloride is brain state dependent and modulates inhibitory neurotransmission in mice. Nat Commun. 2023;14:1871. https://doi.org/10.1038/s41467-023-37433-9.
79. Jeanmonod D, Magnin M, Morel A. Low-threshold calcium spike bursts in the human thalamus. Common physiopathology for sensory, motor and limbic positive symptoms. Brain. 1996;119(Pt 2):363–75. https://doi.org/10.1093/brain/119.2.363.
80. Llinás RR, Steriade M. Bursting of thalamic neurons and states of vigilance. J Neurophysiol. 2006;95:3297–308. https://doi.org/10.1152/jn.00166.2006.
81. Conti D, Bechi Gabrielli G, Panigutti M, Zazzaro G, Bruno G, Galati G, et al. Neuroanatomical and clinical correlates of prodromal dementia with Lewy bodies: a systematic literature review of neuroimaging findings. J Neurol. 2025;272:38. https://doi.org/10.1007/s00415-024-12726-1.
82. Schumacher J, Thomas AJ, Peraza LR, Firbank M, O'Brien JT, Taylor J-P. Functional connectivity of the nucleus basalis of Meynert in Lewy body dementia and Alzheimer's disease. Int Psychogeriatr. 2021;33:89–94. https://doi.org/10.1017/S1041610220003944.
83. Llinás R, Urbano FJ, Leznik E, Ramírez RR, Van Marle HJF. Rhythmic and dysrhythmic thalamocortical dynamics: GABA systems and the edge effect. Trends Neurosci. 2005;28:325–33. https://doi.org/10.1016/j.tins.2005.04.006.
84. Llinás RR, Ribary U, Jeanmonod D, Kronberg E, Mitra PP. Thalamocortical dysrhythmia: a neurological and neuropsychiatric syndrome characterized by magnetoencephalography. Proc Natl Acad Sci U S A. 1999;96:15222–7. https://doi.org/10.1073/pnas.96.26.15222.
85. Arjmandi-Rad S, Vestergaard Nieland JD, Goozee KG, Vaseghi S. The effects of different acetylcholinesterase inhibitors on EEG patterns in patients with Alzheimer's disease: a systematic review. Neurol Sci. 2024;45:417–30. https://doi.org/10.1007/s10072-023-07114-y.
86. Bočková M, Rektor I. Impairment of brain functions in Parkinson's disease reflected by alterations in neural connectivity in EEG studies: a viewpoint. Clin Neurophysiol. 2019;130:239–47. https://doi.org/10.1016/j.clinph.2018.11.013.
87. Babiloni C, Del Percio C, Lizio R, Noce G, Lopez S, Soricelli A, et al. Levodopa may affect cortical excitability in Parkinson's disease patients with cognitive deficits as revealed by reduced activity of cortical sources of resting state electroencephalographic rhythms. Neurobiol Aging. 2019;73:9–20. https://doi.org/10.1016/j.neurobiolaging.2018.08.010.
88. Babiloni C, Cassetta E, Dal Forno G, Del Percio C, Ferreri F, Ferri R, et al. Donepezil effects on sources of cortical rhythms in mild Alzheimer's disease: responders vs. non-responders. Neuroimage. 2006;31:1650–65. https://doi.org/10.1016/j.neuroimage.2006.02.015.

Publisher's Note Springer Nature remains neutral with regard to jurisdictional claims in published maps and institutional affiliations.